NASA TN D-1820

TECHNICAL NOTE

D-1820

TRAJECTORY ENTRY CONDITIONS AT THE LUNAR SPHERE OF INFLUENCE FOR APPLICATION TO DETAILED STUDIES OF NEAR-MOON TRAJECTORY AND IMPACT CONDITIONS

By Harold A. Hamer and Ward F. Hodge

Langley Research Center
Langley Station, Hampton, Va.

NATIONAL AERONAUTICS AND SPACE ADMINISTRATION

WASHINGTON July 1963

NATIONAL AERONAUTICS AND SPACE ADMINISTRATION

TECHNICAL NOTE D-1820

TRAJECTORY ENTRY CONDITIONS AT THE LUNAR SPHERE OF INFLUENCE FOR APPLICATION TO DETAILED STUDIES OF NEAR-MOON TRAJECTORY AND IMPACT CONDITIONS

By Harold A. Hamer and Ward F. Hodge

SUMMARY

Flight conditions at the lunar sphere of influence have been compiled for use in conjunction with detailed studies of earth-moon trajectories. The calculations were based on the assumption that the ascent portion of the trajectory is divided into two parts: one part from earth injection to entry into the sphere of influence (earth-departure trajectory) and the other part lying within this sphere (near-moon trajectory). Each part is approximated by two-body solutions.

In the compilation, trajectory entry conditions at the lunar sphere of influence are presented in relation to earth-injection conditions and essentially describe the complete family of earth-departure trajectories that pass into the sphere of influence. The entry conditions are the vehicle inertial velocity and flight-path angle with respect to the moon and the location of entry around the sphere of influence. These data provide a convenient means of making detailed studies for specified lunar missions without requiring analyses of a large number of earth-departure trajectories. The entry conditions required for a given mission can be established from a detailed study of trajectories within the sphere of influence (simple two-body calculations). The compiled data presented herein correlate these entry conditions to the appropriate earth-injection requirements.

Extensive data pertaining to ballistic trajectories within the sphere of influence have also been presented. In this case, impact conditions (velocity, angle, and location) and perilune altitudes for close-miss trajectories are given in terms of entry conditions at the sphere of influence, and information on time to impact is given for various altitudes above the moon. These data can be used in making detailed studies for lunar-impact or lunar orbital missions.

INTRODUCTION

The planning of circumlunar or lunar landing missions will involve detailed studies of trajectory requisites in the immediate vicinity of the moon. (For

example, see refs. 1 to 3.) Ordinarily, such studies would necessitate investigation of a number of complete trajectories to the moon and, because of the complicated nature of such trajectories, would require extensive calculations. In references 4 and 5 results of comprehensive studies of earth-moon trajectories are presented; however, detailed information regarding trajectory conditions at or near the moon is limited.

This report presents a compilation of pertinent data which eliminates the need for calculating a large number of complete trajectories for use in planning a specific lunar mission. These data relate trajectory conditions at entry into the lunar sphere of influence with corresponding earth-injection conditions. Detailed studies may then be confined to trajectories within the lunar sphere of influence wherein simple two-body calculations apply. In these studies the trajectories may be either ballistic or thrust-augmented, and values of entry conditions required for a specified mission may be readily determined. Data presented in this report, which correlate these values to the earth injection requirements, are then used to establish the complete trajectory from the earth to the moon.

This report also presents data on ballistic impact trajectories and ballistic close-miss trajectories within the lunar sphere of influence. These data are useful for detailed studies of earth-moon missions in which the vehicle is to approach the moon on a collision course or on a low-altitude pass. Lunar impact trajectories are applicable for such missions as research-instrument landing (for example, ref. 6), supply ferry to lunar station, and so forth. Low-altitude (close-miss) trajectories are applicable for establishing orbits about the moon. The impact and near-moon trajectory characteristics are presented in terms of entry conditions at the lunar sphere of influence.

SYMBOLS

The English system of units is used throughout this report. If conversion to metric units is desired, the following relationships apply: 1 foot = 0.3048 meter (exact), and 1 statute mile = 5,280 feet = 1,609.344 meters (exact). Some of the quantities given in this list of symbols are defined geometrically in figures 1, 2, and 3.

A angle between geocentric vehicle velocity vector V_e and selenocentric vehicle velocity vector V_m at entry into lunar sphere of influence, deg

B angle between geocentric radius vector r_e and selenocentric radius vector r_m^* at entry into lunar sphere of influence, deg

C angle between geocentric vehicle velocity vector V_e and tangential orbital velocity vector of moon V_ω at entry into lunar sphere of influence, deg

C_1, C_2 constants of integration (see appendix C)

D	distance between center of earth and center of moon, ft or statute miles
E	eccentric anomaly, radians
F	auxiliary quantity corresponding to the eccentric anomaly in elliptic orbits, radians
l	angular momentum of orbit (per unit mass), ft^2/sec
p	semilatus rectum of orbit, ft
R_m	radius of moon, 5.7024×10^6 ft or 1,080 statute miles
r	radius vector (radial distance from center of earth or moon to vehicle), ft or statute miles
r_m	used in equation (A12) to define distance from center of moon
r_m^*	radius of sphere of influence of moon, ft or statute miles
$r_{m,p}$	perilune distance (from center of moon), statute miles
t	time; sec, min, or days
u	reciprocal of r (see appendix C)
t_p	time to reach perilune of orbit from radial distance r, min
$t_{p,I}$	time to reach perilune of orbit from lunar surface, min
t_I	time to impact moon from radial distance r, $t_p - t_{p,I}$, min
V	vehicle inertial velocity, ft/sec
$V_{i,min}$	minimum vehicle injection velocity to reach moon for given injection radius, ft/sec
ΔV_i	incremental injection velocity, $V_i - V_{i,min}$, ft/sec
V_ω	tangential velocity of moon in assumed circular orbit, ft/sec
X_e, Y_e	inertial rectangular coordinate axes with origin at center of earth (see fig. 1)
X_m, Y_m	inertial rectangular coordinate axes with origin at center of moon (see fig. 1)

α entry angle; angle between line joining centers of earth and moon and selenocentric radius vector at entry into lunar sphere of influence (corresponds to longitude in lunar-orbital plane), deg

γ flight-path angle; angle between velocity vector and line perpendicular to radius vector, deg

ϵ eccentricity of orbit

η angle between geocentric radius vector and line joining centers of earth and moon, deg

θ angle between perigee (perilune) radius vector and geocentric (selenocentric) radius vector, deg

Θ total change in θ for selenocentric orbit, $\theta_m - \theta_I$, deg

λ orientation angle of major axis of earth departure trajectory with respect to line joining centers of earth and moon at injection, deg

μ_e product of universal gravitational constant and mass of earth, ft^3/sec^2

μ_m product of universal gravitational constant and mass of moon, ft^3/sec^2

τ lunar lead angle; angle between geocentric radius vector and line joining centers of earth and moon at injection, deg

ω_m rotational velocity of moon about center of earth, deg/sec or radians/sec

Subscripts:

e geocentric value at entry into lunar sphere of influence

i geocentric value at injection

I selenocentric value at lunar impact

m selenocentric value at entry into lunar sphere of influence

min minimum absolute value for lunar impact

s circular satellite velocity

ASSUMPTIONS AND METHOD

The data in this report, developed from the study of reference 4, are based on the assumption that a sphere of influence exists about the moon. Under this

assumption the earth-to-moon trajectory is separated into two parts, each of which can be determined by simple two-body solutions. The two-body results represent a good approximation of those obtainable from more refined calculations such as from the classic restricted three-body equations of motion. (See ref. 4 for comparison of two-body and three-body results.) A description of the sphere of influence and a derivation of its size (radius of 35,781 statute miles) are given in reference 4.

The calculations apply only to ballistic trajectories; that is, the vehicle inertial velocity or flight-path angle are not altered during flight by additional thrusting. The injection data correspond to launch in an eastward direction with the trajectory of the vehicle lying in the orbital plane of the moon (two-dimensional trajectories). An additional assumption is that the moon revolves about the center of the earth in a circular orbit (average values for the orbital radius and angular velocity of the moon are used).

The equations of motion used to calculate the data are given in appendices A to C. The data are divided into two groups. The first group pertains to the earth-departure trajectory; that is, that part of the trajectory from earth injection to the lunar sphere of influence. (As a necessary inclusion, these data are supplemented with the perilune-distance value of the ensuing selenocentric portion.) The second group pertains to that part of the trajectory within the lunar sphere of influence, the near-moon trajectory. All trajectories in this second group result in lunar ballistic impact or in a close miss of the lunar surface.

Earth-Departure Trajectories

The data for the earth-departure trajectories relate selenocentric entry conditions at the lunar sphere of influence to the earth-injection conditions and to perilune distance (closest approach to the center of the moon of the ensuing near-moon trajectory). The earth injection conditions are defined herein as the flight-path angle γ_i, vehicle inertial velocity V_i, and distance from the center of the earth r_i. For a given combination of these injection conditions the perilune distance depends on the lunar lead angle τ at injection (or time of injection). Lunar-lead-angle data applicable to the present results are presented in reference 4. The selenocentric entry conditions are the flight-path angle γ_m, vehicle inertial velocity V_m, and location around the sphere of influence from the earth-moon line α. Figures 1 and 2 illustrate the various trajectory parameters including those required for converting geocentric (earth) values to selenocentric (moon) values at the sphere of influence.

Some data on entry velocity and entry location for out-of-plane trajectories are given in reference 7. These data indicate that, in general, the two-dimensional results presented herein are good approximations to those obtained for corresponding three-dimensional cases. Specific comparisons between the two sets of data are made subsequently in this report.

Near-Moon Trajectories

The lunar impact velocity V_I, impact angle γ_I, and impact location Θ, as well as close-miss perilune altitude are presented in terms of entry conditions at the lunar sphere of influence. (The data for grazing impacts also represent conditions at close-miss perilunes.) These data used in conjunction with the first group of data (earth-departure trajectories) provide a comprehensive summary of conditions at (or near) the moon and corresponding earth-injection requirements (two-dimensional) for ballistic trajectories. Also included are time-to-impact data for various altitudes above the moon. Figure 3 presents an illustrative sketch showing the pertinent parameters of the near-moon trajectory.

DISCUSSION OF RESULTS

Earth-Departure Trajectories

General.- For any combination of entry conditions at the lunar sphere of influence, the required injection velocity V_i is highly dependent on the injection radius r_i. In order to present the entry data for a range of injection velocities and for a range of injection radii with one set of curves, the results are normalized by plotting the injection velocity in terms of ΔV_i. The quantity ΔV_i is defined as the difference between the injection velocity V_i and the minimum injection velocity required to reach the point on the lunar surface nearest to the earth $V_{i,min}$ $\left(\text{that is, } \Delta V_i = V_i - V_{i,min}\right)$. This manner of normalization is possible since the $V_{i,min}$ values (obtained from ref. 4) are primarily a function of injection radius as shown in figure 4. Hence, for any injection radius (up to at least 4,500 statute miles) the curve shown in figure 4 can be employed to convert the ΔV_i values shown in figures 5 to 10 for earth-departure trajectories to the appropriate V_i values. The normalization procedure gives accurate results in all cases except for entry-velocity data at the higher values of injection radius and injection velocity, as shown subsequently.

The entry conditions are shown (figs. 5 to 10) for the injection-velocity range from the minimum value required to reach the lunar sphere of influence to the value for ΔV_i = 5,000 feet per second. The infinite-velocity value is included where posssible. Injection flight-path angles γ_i are covered over the range from 0° to 60°. The entry conditions are shown for the range of subsequent perilune distances $r_{m,p}$ from zero (dead-center hit) to a value equal to the radius of the lunar sphere of influence. In the latter case, the trajectory just grazes the surface of the sphere of influence.

For a given combination of injection conditions, the lunar lead angle τ (or injection time) determines whether the earth-departure trajectory will be "ascending" or "decending" and the entry conditions are shown in figures 5 to 10 for both cases. Ascending trajectories reach perilune while the vehicle is still moving away from the earth; the opposite is true for descending trajectories.

Descending trajectories would ordinarily be considered impractical because of the comparatively longer trip times to the sphere of influence. However, this type of trajectory does afford entry locations not attainable with ascending trajectories. The descending-trajectory data are shown only for injection velocities well below the earth escape value; values of ΔV_i higher than 162 feet per second result in trajectories which would extend beyond the terrestrial sphere of influence in the sun-earth system and would thus be affected by the gravitational attraction of the sun. (See ref. 4 for complete description of lunar-trajectory characteristics.)

The lunar lead angle also determines whether the direction around the moon (within the sphere of influence) will be clockwise or counterclockwise. Therefore, in addition to classifying the entry-condition data according to ascending or descending earth-departure trajectories, the data are classified according to the direction around the moon. The direction is shown as seen from the celestial north pole. It should be noted that for counterclockwise motion the vehicle never passes completely around the side of the moon farthest from the earth.

Entry-flight-path angle.- The values of flight-path angle at entry into the lunar sphere of influence are presented in figure 5. Entry-flight-path angle is shown to be primarily a function of perilune distance $r_{m,p}$ (or injection time); there is also a small effect due to injection velocity. Also evident in figure 5 is the fact that only a relatively small range of entry angles (approximately -85° to -95°) leads to ballistic impact of the moon.

The curve in figure 5(a) represents the entry angles for comparatively low injection velocities; that is, from the minimum value required to reach the point on the lunar sphere of influence nearest to the earth (ΔV_i slightly less than -45 ft/sec) to a ΔV_i value of 45 feet per second. The latter value corresponds approximately to the minimum injection velocity required to reach the point on the sphere of influence farthest from the earth. Because of slight variations in the data, the single curve drawn to represent the velocity range covered in figure 5(a) is accurate to only within $\pm 1^\circ$. As noted, the entry angles in figure 5(a) apply to either ascending or descending earth-departure trajectories. Each limit shown on the curve indicates that portion of the curve that applies to the corresponding injection velocity. For example, for an injection velocity corresponding to $\Delta V_i = -30$ feet per second, the closest approach to the center of the moon $r_{m,p}$ can be anywhere from 35,781 to about 22,000 miles, depending on the lunar lead angle at injection. These perilunes lie in the portion of the sphere of influence nearest to the earth. For $\Delta V_i = 30$ feet per second, the value of $r_{m,p}$ can be anywhere from 35,781 to 0 miles for perilunes in the near portion of the sphere of influence, but only from 0 to 20,000 miles for perilunes in the far portion.

Data in figure 5(b) can be used to determine the entry angles for earth-departure trajectories in the region of the higher elliptic-injection velocities as well as for all those in the hyperbolic region. Only the curve shown for $\Delta V_i = 100$ feet per second is valid for descending trajectories. As previously noted, descending trajectories that correspond to a ΔV_i greater than 162 feet per second are not considered in the present analysis.

Entry velocity.- The data in figures 6 to 8 apply to vehicle velocity (with respect to the moon) at entry into the lunar sphere of influence. As shown by each ΔV_i curve in figures 6 and 7, the entry velocity V_m varies according to perilune distance (or injection time). Cross plots of the data in either figure 6 or figure 7 will yield entry velocity for any given injection velocity up to ΔV_i = 5,000 feet per second. The normalization procedure (that is, plotting the data in terms of ΔV_i) does not result in making the entry velocity entirely independent of the injection radius. The entry-velocity data are shown in figures 6 and 7 for an injection radius of 4,100 miles (140-mile altitude) and can be converted (corrected) to apply to any other injection radius by information presented in figure 8. (As shown in figure 8, the variation of the correction value with injection radius is approximately linear at any value of injection velocity. Figure 8 also applies to injection radii less than 4,100 miles, in which case the correction will be a positive value.)

The entry velocity has a slight dependence on whether the trajectory is ascending or descending, as shown in figures 6 and 7. In figure 7 (descending trajectories) the range of applicable injection velocities extends only to ΔV_i = 162 feet per second, as has been previously discussed. The difference in entry velocity between the ascending and descending trajectories varies from 0 to about 120 feet per second depending on the value of V_i and $r_{m,p}$. For lunar impact ($r_{m,p}$ = 1,080 miles) this difference is approximately zero.

Data in figures 6 and 7 are shown for four specific values of injection flight-path angle over the range from 0° to 60°. For low values of γ_i (0° to 20°), the entry-velocity data are practically the same; however, at the higher values of γ_i (40° and 60°) there is some noticeable difference in the data, especially in the low-velocity range.

The limit lines shown in figures 6 and 7 correspond to the lowest entry velocities possible for ballistic trajectories emanating from the earth. It is of interest to note that for a given combination of earth-injection conditions (V_i, γ_i, and r_i), the entry velocity will have a range of about 1,000 feet per second according to the value of $r_{m,p}$ and the direction of the ensuing selenocentric portion of the trajectory.

An indication of how closely the velocity data for the two-dimensional case (coplanar) presented herein apply to the three-dimensional case (trajectory out of earth-moon plane) is available from reference 7. Data in this reference show that differences in entry velocity (with respect to the moon) at the sphere of influence between in-plane trajectories and trajectories inclined up to 30° to the earth-moon plane are less than 100 feet per second.

Entry location.- Data for location of the entry into the lunar sphere of influence (figs. 9 and 10) are given with respect to the earth-moon line at entry. The location angle α (illustrated in figs. 1 and 2) is measured positive in the counterclockwise direction (as seen from celestial north pole) and corresponds to

longitude in the lunar-orbital plane. These data can be applied to the determination of lunar-impact location or perilune location.

As noted in figures 9 and 10, the results apply to any injection altitude. Also, the data are shown for four specific values of injection flight-path angle over the range from 0° to 60°. For low values of γ_i (0° to 20°), the entry-longitude data are practically the same; at the higher values of γ_i (40° and 60°) there is some noticeable difference in the data.

As shown in figure 9, entry longitudes for ascending trajectories are not attainable in the range $\alpha = 80^\circ$ to 180°, whereas for descending trajectories (fig. 10) this range is 0° to 140°. The entry-longitude range of 80° to 140° is not attainable from earth-departure trajectories, or more practically, the range 80° to 180°, since the region 140° to 180° corresponds to trajectories with long trip times.

A comparison of the two-dimensional results presented herein with the results of reference 7 shows that differences in entry longitude (measured in lunar-orbital plane) between in-plane trajectories and trajectories inclined up to 30° to the earth-moon plane are not more than 1°.

Near-Moon Trajectories

General.- Figures 11 to 16 pertain to trajectories within the lunar sphere of influence. Any ballistic trajectory emanating from the earth enters the sphere of influence at hyperbolic velocity with respect to the moon. The calculations for the conditions at or near the moon, therefore, pertain to hyperbolic trajectories within the lunar sphere of influence. The lower values of hyperbolic velocity (less than about 2,700 ft/sec) are not achievable at entry with ballistic trajectories from the earth, but could be obtained by midcourse thrusting (at the surface of the sphere of influence) or from trajectories emanating from some other source. Thus, as a matter of completeness, data are included for the entire hyperbolic range of entry velocities from parabolic (escape) to infinite velocity. The value shown for the minimum entry velocity for earth injection was obtained from figure 6 or 7 and corresponds to a ballistic trajectory that will just reach the moon ($r_{m,p}$ = 1,080 miles). (A lower minimum value of about 2,640 ft/sec is achievable by just grazing the sphere of influence ($r_{m,p}$ = 35,781 miles).)

The entry flight-path angle γ_m can have any value from 0° to -180°; however, for a given entry velocity, lunar impact (or perilune passage within several hundred miles) can occur only within a limited range of entry-flight-path angles. The end points of the impact range correspond to tangential or "grazing" impacts (perilune distance equal to the radius of the moon), and its midpoint forms a dividing line between clockwise and counterclockwise motion about the moon. Since the motion is symmetrical about this line, it is sufficient for the purposes of this report to present impact data only for the clockwise region of motion. The extremities of this clockwise region are designated as impact boundaries: one which corresponds to tangential impacts, and the other to radial or

"dead-center" impacts for which the flight-path angle along the trajectory remains constant at -90°. Similarly, the close-miss data (perilune altitudes) are presented only for clockwise motion.

Impact velocity.- The impact velocity is related to the entry velocity through the principle of conservation of energy (eq. (B7a)). The variation in impact velocity with entry velocity is presented in figure 11. The resulting curve is one branch of a hyperbola which becomes asymptotic to a 45° line through the origin as the velocity becomes infinite. The minimum impact velocity corresponds to a free fall from rest at the boundary of the sphere of influence to the surface of the moon and was calculated by using equation (B7b).

Limitations on entry-flight-path angle for impact.- For a given value of entry velocity, the minimum (absolute) value of γ_m for lunar impact results in a tangential (grazing) impact. A simple equation for calculating this minimum entry-flight-path angle for impact $\gamma_{m,min}$ is obtained directly from the principle of conservation of angular momentum, as follows:

$$l = r_m{}^* V_m \cos \gamma_m = R_m V_I \cos \gamma_I$$

By solving for γ_m and noting that $\gamma_I = 0$ at perilune, the following equation for $\gamma_{m,min}$ is obtained:

$$\gamma_{m,min} = \cos^{-1}\left(\frac{R_m V_I}{r_m{}^* V_m}\right)$$

This equation results in the curve shown in figure 12. As indicated in figure 12, $\gamma_{m,min}$ reaches a maximum (negative) value of about -88.27° as V_m becomes infinite. This extremum of $\gamma_{m,min}$ is equal to the complement of half the angle subtended by the moon at the boundary of the sphere of influence.

Impact angle.- The impact flight-path angle is plotted against entry flight-path angle in figure 13. This plot includes data for the entire range of hyperbolic velocities within the sphere of influence. Parabolic or escape velocity forms a lower limit on the entry velocity and infinite velocity forms the upper limit. The equations given in appendix B are not valid for infinite velocity; however, the infinite velocity curve is easily calculated by means of simple trigonometry. The two impact boundaries are also included in figure 13. The radial impact boundary appears simply as a point common to all curves since the flight-path angle along the trajectory remains constant at -90° for all entry velocities. Data from figure 12 form the tangential impact boundary which coincides with the γ_m-axis since γ_I must be zero at perilune.

Impact location.- In figure 14, the total change in the angle θ is plotted against γ_m for the hyperbolic range of values of V_m. This change in angle Θ

is equivalent to the total angular travel around the moon from entry to impact. The same limits and boundaries discussed in figure 13 are included in this plot. The radial impact boundary is the point common to all curves and the tangential impact boundary becomes a curve defined by the data of figure 12. As in figure 13, the infinite velocity curve was obtained by means of simple trigonometry.

If the inclination of the near-moon trajectory plane is known and the axial rotation of the moon is accounted for, the angle Θ can be used to determine the approximate longitude and latitude of impact with respect to coordinate axes fixed at the center of the moon. A suitable lunar coordinate system in which the X-axis is toward the direction of the earth through the lunar equatorial bulge at Sinus Medii (Central Bay), the Z-axis along the axis of rotation, and the Y-axis orthogonal to the X,Z plane is described in reference 8. In this coordinate system, zero longitude and latitude are located at Sinus Medii. Since this is an equatorial coordinate system, only the longitude of impact will be affected by the axial rotation of the moon. If the time to impact, which is discussed in the next section, is known, the product of the time to impact and the angular velocity of the moon about its axis of rotation will give the correction in longitude which is to be subtracted if the motion is in the direction of the moon rotation or to be added if opposite it.

Time to impact.- For studies of the near-moon portions of earth-to-moon trajectories, data on time to impact the moon is of interest. One use of such data, that of determining lunar equatorial impact longitude, was discussed in the preceding section. For a manned mission, data on the variation in the time to impact as the vehicle approaches the moon would be important in connection with navigation, retrofiring procedures, and so forth.

The time required to impact the moon is plotted against γ_m and V_m in figure 15 for altitudes ranging from the surface of the sphere of influence down to 5,000 statute miles. As in the preceding figures, both impact boundaries and both velocity limits appear on the plots. Figure 15 shows that the impact time has a much stronger dependence on V_m than on γ_m and, in general, decreases as V_m increases. However, a "cross-over" in the tangential impact boundary appears in figure 15(d). The data of figure 15(d) indicate that the remaining time until impact is greater for a higher entry velocity than for a lower one in the region to the right of the cross-over point. The reason for this apparent paradox can be explained with the aid of figure 14 which shows that for all values of γ_m, the angle Θ becomes progressively larger as V_m is increased. This result means that for a given value of γ_m, the total distance along the trajectory increases with V_m. Thus, the ratio of the remaining distances to be traveled for two different values of V_m will increase as the altitude decreases. When the altitude becomes small enough, the remaining distance to be traveled at the higher velocity is sufficiently greater than the corresponding distance for the lower velocity; thus the remaining time until impact is accordingly larger in the cross-over region. For altitudes less than 5,000 statute miles above the lunar surface, this cross-over effect becomes progressively more pronounced. However, figure 15 was not plotted for altitudes less than 5,000 miles since the remaining time to impact becomes relatively small. At an altitude of 1,000 miles,

the remaining time is roughly 18 to 20 minutes for most of the velocity range and at 500 miles, the time left is only 6 to 10 minutes.

Perilune altitudes for close-miss trajectories.- Manned lunar missions will ordinarily require the establishment of orbits close to the moon. Transfer from the hyperbolic trajectory into a circular orbit will probably occur at perilune altitude (closest approach to lunar surface). The data relating perilune altitude to entry conditions are presented in figure 16 for a range of altitudes to 900 miles. Perilune radii were calculated from

$$r_{m,p} = \frac{p_m}{1 + \epsilon_m}$$

where p_m and ϵ_m are related to the entry conditions. (See appendix B.) The perilune altitude is shown to be highly sensitive to entry flight-path angle.

The velocity at perilune and perilune location from entry are not included; however, the data presented herein for tangential impact will closely approximate these values for close-miss trajectories. The velocity at perilune can be calculated from equation (B7a) by replacing R_m by $r_{m,p}$ and the perilune location is given by equation (B3).

CONCLUDING REMARKS

A purpose of this report has been to present an extensive collection of data relating the trajectory entry conditions at the lunar sphere of influence to earth-injection conditions (earth-departure trajectories). These data used in conjunction with detailed studies of trajectories within the sphere of influence (near-moon trajectories) provide a convenient means of determining earth-injection requirements for specified lunar missions.

The results are based on two-body solutions but are good approximations to those obtained by more refined methods of trajectory computation. Also, the results refer specifically to trajectories launched in the earth-moon plane, but are generally applicable to out-of-plane trajectories.

Also included in this report are comprehensive data on near-moon trajectories that will apply in making detailed studies for lunar-impact or lunar orbital missions. Use of these data in conjunction with the data for earth-departure trajectories provides a complete summary of conditions at or near the moon and corresponding earth-insertion requirements.

Langley Research Center,
National Aeronautics and Space Administration,
Langley Station, Hampton, Va., April 12, 1963.

APPENDIX A

EQUATIONS FOR EARTH-DEPARTURE TRAJECTORY

The equations of motion for the earth-departure trajectory; that is, that part of the trajectory to the lunar sphere of influence, are presented in this appendix. Also included are the equations for converting geocentric (earth) trajectory values to selenocentric (moon) values at the surface of the sphere of influence. Figures 1 and 2 show the directions for the angles and aid in visualizing the equations.

The basic assumptions used for these equations have been discussed in the main body of the report. Because of the magnitude of the equation constants in English units, it was convenient to perform the calculations in lunar units. In addition, time was taken in terms of days. The computed results were then converted to English units. The constants are given in table I in both English and lunar units for the moon at an average distance from the earth.

Two-Body Equations

For computing the earth-departure trajectory (which may be either elliptic, parabolic, or hyperbolic), the distance from the center of the earth for any given value of θ is:

$$r = \frac{p_i}{1 + \epsilon_i \cos \theta} \tag{A1}$$

where θ is measured counterclockwise from the perigee radius vector to the vehicle radius vector of the point in question. The semilatus rectum of the departure trajectory is:

$$p_i = r_i \left(\frac{V_i}{V_{s,i}} \right)^2 \cos^2 \gamma_i \tag{A2}$$

where r_i is the injection radius vector from the center of the earth, V_i is the injection inertial velocity, γ_i is the injection inertial flight-path angle measured with respect to the local spherical horizontal, and circular satellite velocity at r_i is

$$V_{s,i} = \sqrt{\frac{\mu_e}{r_i}} \tag{A3}$$

The eccentricity of the earth-departure trajectory is

$$\epsilon_i = \frac{1}{\cos \theta_i}\left(\frac{p_i}{r_i} - 1\right) \tag{A4}$$

where

$$\tan \theta_i = \tan \gamma_i\left[\frac{p_i/r_i}{(p_i/r_i) - 1}\right] \tag{A5}$$

For computing the inertial velocity at any point in the earth-departure trajectory,

$$V = \sqrt{\mu_e\left(\frac{2}{r} - \frac{1 - \epsilon_i^2}{p_i}\right)} \tag{A6}$$

where r is the distance from the center of the earth. For computing the inertial flight-path angle at any point,

$$\tan \gamma = \frac{\epsilon_i \sin \theta}{1 + \epsilon_i \cos \theta} \tag{A7}$$

For computing the time from injection to any point,

$$t = t(\theta) - t(\theta_i) \tag{A8}$$

where $t(\theta)$ is time from perigee to the point in question, and $t(\theta_i)$ is the time from perigee to injection. The value of $t(\theta)$ is computed as follows:

If $\epsilon_i < 1$ (elliptic trajectory),

$$t(\theta) = \frac{p_i}{1 - \epsilon_i^2}\sqrt{\frac{p_i}{\mu_e}}\frac{1}{\sqrt{1 - \epsilon_i^2}}(E - \epsilon_i \sin E) \tag{A9}$$

where E is the eccentric anomaly and

$$\tan \frac{E}{2} = \sqrt{\frac{1 - \epsilon_i}{1 + \epsilon_i}} \tan \frac{\theta}{2} \tag{A9a}$$

If $\epsilon_i > 1$ (hyperbolic trajectory),

$$t(\theta) = \frac{p_i}{\epsilon_i^2 - 1}\sqrt{\frac{p_i}{\mu_e}}\frac{1}{\sqrt{\epsilon_i^2 - 1}}(-F + \epsilon_i \sinh F) \tag{A10}$$

where F is an auxiliary quantity in hyperbolic orbits corresponding to the eccentric anomaly in elliptic orbits, and

$$\tanh \frac{F}{2} = \sqrt{\frac{\epsilon_i - 1}{\epsilon_i + 1}} \tan \frac{\theta}{2} \tag{A10a}$$

If $\epsilon_i = 1$ (parabolic trajectory),

$$t(\theta) = p_i \sqrt{\frac{p_i}{\mu_e}}\left(\frac{1}{2} \tan \frac{\theta}{2}\right)\left(1 + \frac{1}{3} \tan^2 \frac{\theta}{2}\right) \tag{A11}$$

The value of $t(\theta_i)$ is computed by using the appropriate equation (eq. (A9), (A10), or (A11)) and by substituting θ_i for θ. It should be noted that if injection is at perigee the value of $t(\theta_i)$ will be zero. Also, the angles $E/2$ and $F/2$ in equations (A9a) and (A10a) should always be considered to be in the same quadrant as $\theta/2$.

An important step in the calculations is to determine the point of entry of the departure trajectory into the lunar sphere of influence. The method used in this study was an iteration process which at a given value of θ compared the distance from the center of the moon r_m with the radius of the lunar sphere of influence r_m^* and computed the value of θ necessary to make this difference zero. This value, then, is taken as θ_e. The equation used to calculate the distance from the center of the moon was

$$r_m^2 = D^2 + r^2 - 2rD \cos \eta \tag{A12}$$

where r is the distance from the center of the earth to the point on the trajectory under consideration and η is the angle between the radius vector from the earth and the line joining the centers of the earth and moon. The angle η is computed from the following equation:

$$\eta = \theta + \lambda - \omega_m t - 180^\circ \tag{A13}$$

The angle λ is related to the lunar lead angle τ by the following equation:

$$\lambda = 180^\circ - \theta_i - \tau \tag{A14}$$

where the lunar lead angle is the angle between the radius vector and a line joining the centers of the earth and moon at injection.

Once the value of θ is determined at the point of entry into the sphere of influence, the geocentric values of r, V, γ, and η can be readily calculated for this point. These values are defined as r_e, V_e, γ_e, and η_e. It should be noted that at this point

$$\sin \eta_e \leqq \frac{r_m^*}{D} \tag{A15}$$

and

$$\left(D - r_m^*\right) \leqq r_e \leqq \left(D + r_m^*\right) \tag{A16}$$

The location of entry around the sphere of influence, defined by the angle α, is:

$$\alpha = \eta_e + B \tag{A17}$$

where the equation for the angle B is given in the subsequent section.

Equations for Converting to Moon Coordinates

For converting velocity and flight-path angle at the point of entry to selenocentric values, the distance from the center of the moon is r_m^*. The velocity at entry with respect to the moon is

$$V_m^2 = V_e^2 + V_\omega^2 - 2V_eV_\omega \cos C \tag{A18}$$

where V_e is the geocentric value at entry, the tangential velocity of the moon rotating about the earth is

$$V_\omega = D\omega_m \tag{A19}$$

and the angle C is

$$C = \gamma_e - \eta_e \tag{A20}$$

where γ_e and η_e are the geocentric values at entry. The flight-path angle at entry with respect to the moon is

$$\gamma_m = -B + A - \gamma_e \tag{A21}$$

where

$$\sin B = \frac{-\sin \eta_e}{r_m^*/D} \tag{A22}$$

and

$$\sin A = -\frac{V_\omega}{V_m} \sin C \tag{A23}$$

In order that B and A will be in the proper quadrant, the following two rules may be used:

(1) The sign of cos B is the sign of the quantity

$$D^2 - r_e^2 - \left(r_m^*\right)^2$$

(2) The sign of cos A is the sign of the quantity

$$V_e^2 + V_m^2 - V_\omega^2$$

APPENDIX B

EQUATIONS FOR NEAR-MOON TRAJECTORY

The equations of motion used in calculating position and velocity data for trajectories within the lunar sphere of influence are presented in this appendix. The equations are expressed in terms of the entry conditions at the surface of the sphere of influence since all trajectories are assumed to originate at that point. Also, the equations refer specifically to impact conditions, but will apply to conditions at any distance from the moon. The first two equations define constants of the motion, which are the semilatus rectum

$$p_m = \frac{\left(r_m^* V_m \cos \gamma_m\right)^2}{\mu_m} \tag{B1}$$

and the eccentricity

$$\epsilon_m = \frac{1}{\cos \theta_m}\left(\frac{p_m}{r_m^*} - 1\right) \tag{B2}$$

Additional two-body equations used in the calculations are:

$$\tan \theta_m = \tan \gamma_m \left[\frac{p_m / r_m^*}{\left(p_m / r_m^*\right) - 1}\right] \tag{B3}$$

$$\cos \theta_I = \frac{1}{\epsilon_m}\left(\frac{p_m}{R_m} - 1\right) \tag{B4}$$

$$\Theta = \theta_m - \theta_I \tag{B5}$$

$$\tan \gamma_I = \frac{\epsilon_m R_m \sin \theta_I}{p_m} \tag{B6}$$

$$V_I = \sqrt{\mu_m\left(\frac{2}{R_m} - \frac{1 - \epsilon_m^2}{p_m}\right)} \tag{B7}$$

$$V_I = \sqrt{\frac{2\mu_m}{R_m} + V_m^2 - \frac{2\mu_m}{r_m^*}} \tag{B7a}$$

For the minimum impact velocity, which corresponds to a free fall to the lunar surface from the boundary of the sphere of influence, V_m is zero and equation (B7a) becomes

$$V_I = \sqrt{2\mu_m\left(\frac{1}{R_m} - \frac{1}{r_m^*}\right)} \tag{B7b}$$

In the special case where V_m equals the escape or parabolic velocity, $V_m^2 = \frac{2\mu_m}{r_m^*}$ and equation (B7a) reduces to

$$V_I = \sqrt{\frac{2\mu_m}{R_m}} \tag{B7c}$$

APPENDIX C

EQUATIONS FOR TIME TO IMPACT

This appendix contains the equations used for calculating time-to-impact data relating to trajectories within the lunar sphere of influence. The methods used to develop these equations are essentially those given in reference 9.

An expression for the time to reach perilune for hyperbolic motion can be derived as follows. Resolve the velocity (as defined by eq. (B7)) into its radial and tangential components expressed in differential form

$$\left(\frac{dr}{dt}\right)^2 + \left(r\frac{d\theta}{dt}\right)^2 = \mu_m\left(\frac{2}{r} - \frac{1 - \epsilon_m^2}{p_m}\right)$$

where θ is the angle measured from the perilune radius vector to the vehicle selenocentric radius vector r for any given point on the trajectory. Solving for dt

$$dt = \left[\frac{(dr)^2 + r^2(d\theta)^2}{\mu_m\left(\frac{2}{r} - \frac{1 - \epsilon_m^2}{p_m}\right)}\right]^{1/2}$$

Differentiate equation (B7) with respect to θ and use the result to eliminate dr from this equation. This step yields the following expression for the differential time:

$$dt = \frac{p_m^{3/2}}{\sqrt{\mu_m}}\left[\frac{d\theta}{(1 + \epsilon_m \cos\theta)^2}\right]$$

which can be integrated with tables in two steps to give

$$t_p = \sqrt{\frac{p_m}{\mu_m}}\left(\frac{p_m}{1 - \epsilon_m^2}\right)\left[\frac{-\epsilon_m \sin\theta}{1 + \epsilon_m \cos\theta} + \frac{2}{\sqrt{\epsilon_m^2 - 1}} \tanh^{-1}\left(\frac{\sqrt{\epsilon_m^2 - 1}}{\epsilon_m + 1} \tan\frac{\theta}{2}\right)\right]$$

By using trigonometric identities, this equation can be more conveniently expressed as

$$t_p = \sqrt{\frac{p_m}{\mu_m}}\left(\frac{p_m}{\epsilon_m^2 - 1}\right)\left[\frac{\epsilon_m \sin\theta}{1 + \epsilon_m \cos\theta} - \frac{1}{\sqrt{\epsilon_m^2 - 1}} \log_e\left(\frac{\epsilon_m + \cos\theta + \sqrt{\epsilon_m^2 - 1}\sin\theta}{1 + \epsilon_m \cos\theta}\right)\right] \quad \text{(C1)}$$

Inspection of this equation shows that it does not hold for parabolic or for radial motion. Time equations which are valid at the impact boundaries and velocity limits discussed in this report can be derived as follows:

An equation for the time to reach perilune for parabolic motion can be obtained by integrating a differential form of the equation for angular momentum. The resulting equation is

$$t_p = \frac{p_m}{2}\sqrt{\frac{p_m}{\mu_m}}\left(\tan\frac{\theta}{2} + \frac{1}{3}\tan^3\frac{\theta}{2}\right) \tag{C2}$$

Except for radial motion, equations (C1) and (C2) cover all cases of parabolic and hyperbolic motion and both are valid at the tangential impact boundary. Since these equations give the time to reach perilune of the orbit, the time to impact is given by

$$t_I = t_p - t_{p,I} \tag{C3}$$

where t_p and $t_{p,I}$ are determined by substituting the appropriate values of θ into equation (C1) or (C2).

The remaining case to consider is motion toward the moon along the radial impact boundary. Here the tangential component of the velocity is always zero and an expression for the time to impact can be derived from equation (B7a) by writing it in the following differential form which can be integrated as indicated:

$$\frac{dr}{dt} = \sqrt{\frac{2\mu_m}{r} + C_1}$$

where

$$C_1 = V_m^2 - \frac{2\mu_m}{r_m^*}$$

Separating the variables and making the substitution $u = 1/r$ gives

$$dt = \frac{dr}{\sqrt{\frac{2\mu_m}{r} + C_1}}$$

$$= -\frac{du}{u^2\sqrt{2\mu_m u + C_1}}$$

The results of the integration yield

$$t = \frac{\sqrt{2\mu_m u + C_1}}{C_1 u} + \frac{\mu_m}{C_1} \int \frac{du}{u\sqrt{2\mu_m u + C_1}} + C_2 \qquad (C4)$$

which constitute a general solution to the problem. The form in which the second integral in equation (C4) is evaluated depends on the value of C_1 which determines whether the motion is hyperbolic, parabolic, or elliptic.

For the case of radial motion at hyperbolic velocity, $C_1 > 0$ and equation (C4) becomes

$$t = \frac{\sqrt{2\mu_m u + C_1}}{C_1 u} + \frac{\mu_m}{C_1\sqrt{C_1}} \log_e\left(\frac{\sqrt{2\mu_m u + C_1} - \sqrt{C_1}}{\sqrt{2\mu_m u + C_1} + \sqrt{C_1}}\right) + C_2$$

$$= \frac{rV}{C_1} + \frac{\mu_m}{C_1\sqrt{C_1}} \log_e\left(\frac{V - \sqrt{C_1}}{V + \sqrt{C_1}}\right) + C_2$$

By using the initial conditions $r = r_m^*$ and $V = V_m$ when $t = 0$ to evaluate C_2, the following equation is obtained for time to impact from the surface of the sphere of influence:

$$t_I = \frac{1}{C_1}\left\{\left(R_m V_I - r_m^* V_m\right) + \frac{\mu_m}{\sqrt{C_1}}\left[\log_e\left(\frac{V_I - \sqrt{C_1}}{V_I + \sqrt{C_1}}\right) - \log_e\left(\frac{V_m - \sqrt{C_1}}{V_m + \sqrt{C_1}}\right)\right]\right\} \qquad (C4a)$$

For the parabolic case, $C_1 = 0$ and equation (B7a) reduces to

$$\frac{dr}{dt} = \sqrt{\frac{2\mu_m}{r}}$$

which can be integrated by simple quadrature to give

$$t = \frac{1}{3} r^{3/2} \sqrt{\frac{2}{\mu_m}} + C_2$$

which reduces to the following equation for time to impact from the surface of the sphere of influence:

$$t_I = \frac{1}{3}\sqrt{\frac{2}{\mu_m}}\left[(r_m^*)^{3/2} - (R_m)^{3/2}\right] \qquad (C4b)$$

where C_2 has been evaluated using the initial condition $r = r_m^*$ when $t = 0$.

For the elliptic case, $C_1 < 0$ and equation (C4) takes the form

$$t = \frac{\sqrt{2\mu_m u + C_1}}{C_1 u} + \frac{2\mu_m}{C_1\sqrt{-C_1}} \tan^{-1}\sqrt{\frac{2\mu_m u + C_1}{-C_1}} + C_2$$

which gives

$$t_I = \frac{1}{C_1}\left\{\left(R_m V_I - r_m^* V_m\right) + \frac{2\mu_m}{\sqrt{-C_1}}\left[\tan^{-1}\left(\frac{V_I}{\sqrt{-C_1}}\right) - \tan^{-1}\left(\frac{V_m}{\sqrt{-C_1}}\right)\right]\right\} \qquad (C4c)$$

when C_2 is evaluated as in equation (C4a).

As a matter of interest, it might be noted that equation (C4c) can be used to calculate the time to fall freely to the lunar surface from a position of rest. In this case, V_m is zero and $C_1 = -\frac{2\mu_m}{r_m^*}$.

REFERENCES

1. Weber, Richard J., and Pauson, Werner M.: Some Thrust and Trajectory Considerations For Lunar Landings. NASA TN D-134, 1959.

2. Jenkins, Morris V., and Munford, Robert E.: Preliminary Survey of Retrograde Velocities Required for Insertion Into Low-Altitude Lunar Orbits. NASA TN D-1081, 1961.

3. Nelson, Walter C.: The Selection of Lunar Trajectories. [Preprint] 2077-61, American Rocket Soc., Oct. 1961.

4. Huss, Carl R., Hamer, Harold A., and Mayer, John P.: Parameter Study of Insertion Conditions for Lunar Missions Including Various Trajectory Considerations. NASA TR R-122, 1961.

5. Hiller, H.: A Generalised Study of Two-Dimensional Trajectories of a Vehicle in Earth-Moon Space. Tech. Note. No. Space 2, British R.A.E., Jan. 1962.

6. Nicks, Oran W.: The Role of Project Ranger in the NASA Lunar Program. [Preprint] 2236-61, American Rocket Soc., Oct. 1961.

7. Tolson, Robert H.: Geometrical Characteristics of Lunar Orbits Established From Earth-Moon Trajectories. NASA TN D-1780, 1963.

8. Kalensher, B. E.: Selenographic Coordinates. Tech. Rep. No. 32-41 (Contract No. NASw-6), Jet Propulsion Lab., C.I.T., Feb. 24, 1961.

9. Moulton, Forest Ray: An Introduction to Celestial Mechanics. Second rev. ed., The Macmillan Co., c.1914.

TABLE I.- CONSTANTS FOR AVERAGE EARTH-TO-MOON DISTANCE

	English units	Lunar units
Distance between center of earth and center of moon, D	1,261,164,960 ft or 238,857 statute miles	1 lunar unit
Rotational velocity of moon about center of earth, ω_m	0.00015250415 deg/sec or 0.0000026616995 radian/sec	13.17635854 deg/day or 0.22997084 radian/day
Product of universal gravitational constant and mass of earth, μ_e	1.4077×10^{16} ft^3/sec^2	0.052386804 $(\text{lunar units})^3/day^2$
Product of universal gravitational constant and mass of moon, μ_m	1.7282996×10^{14} ft^3/sec^2	0.0006431775 $(\text{lunar units})^3/day^2$
Radius of sphere of influence of moon, r_m*	188,923,680 ft or 35,781 statute miles	0.1498 lunar unit

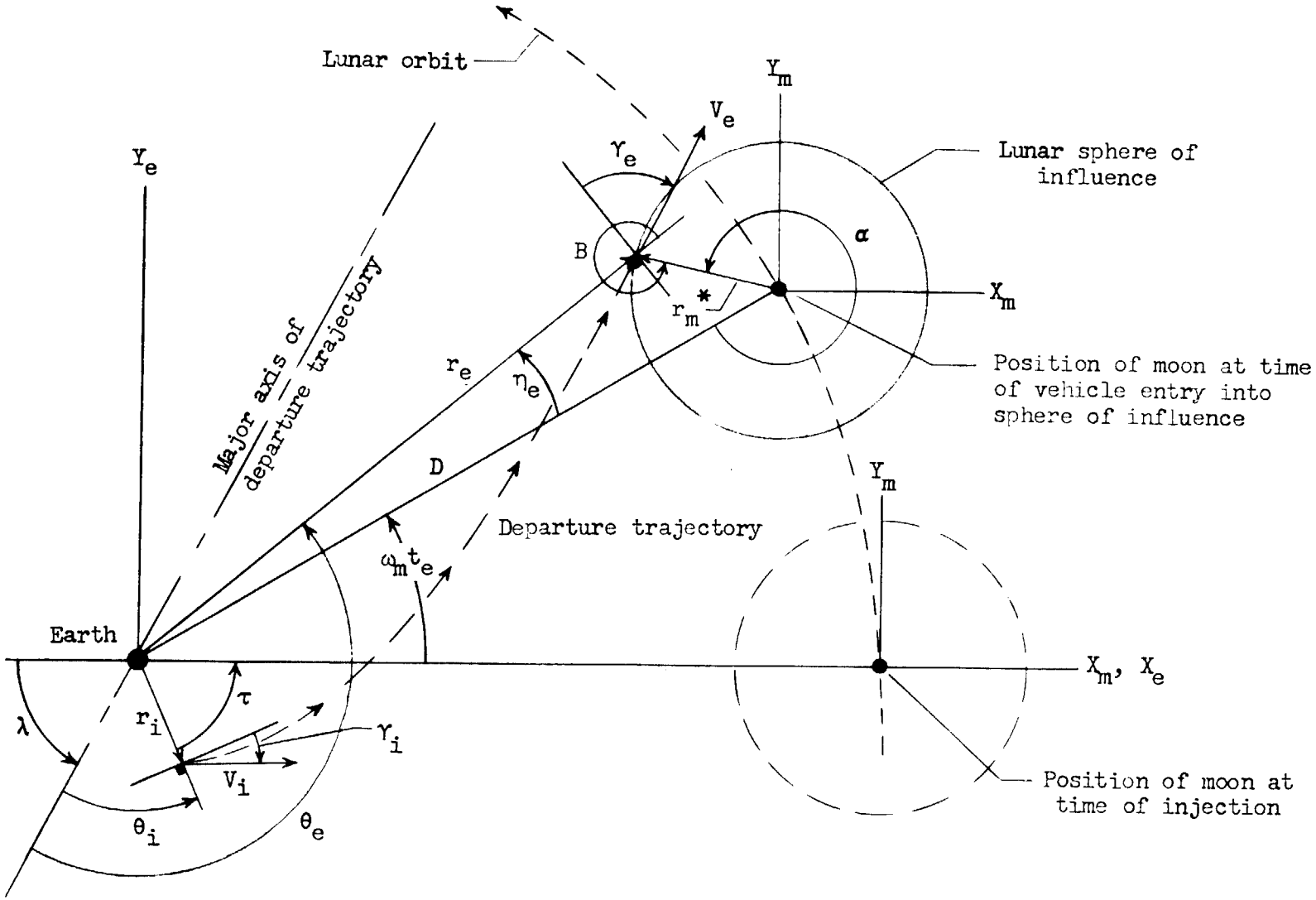

Figure 1.- Sketch showing definition of parameters for earth-departure trajectory. Positive directions shown.

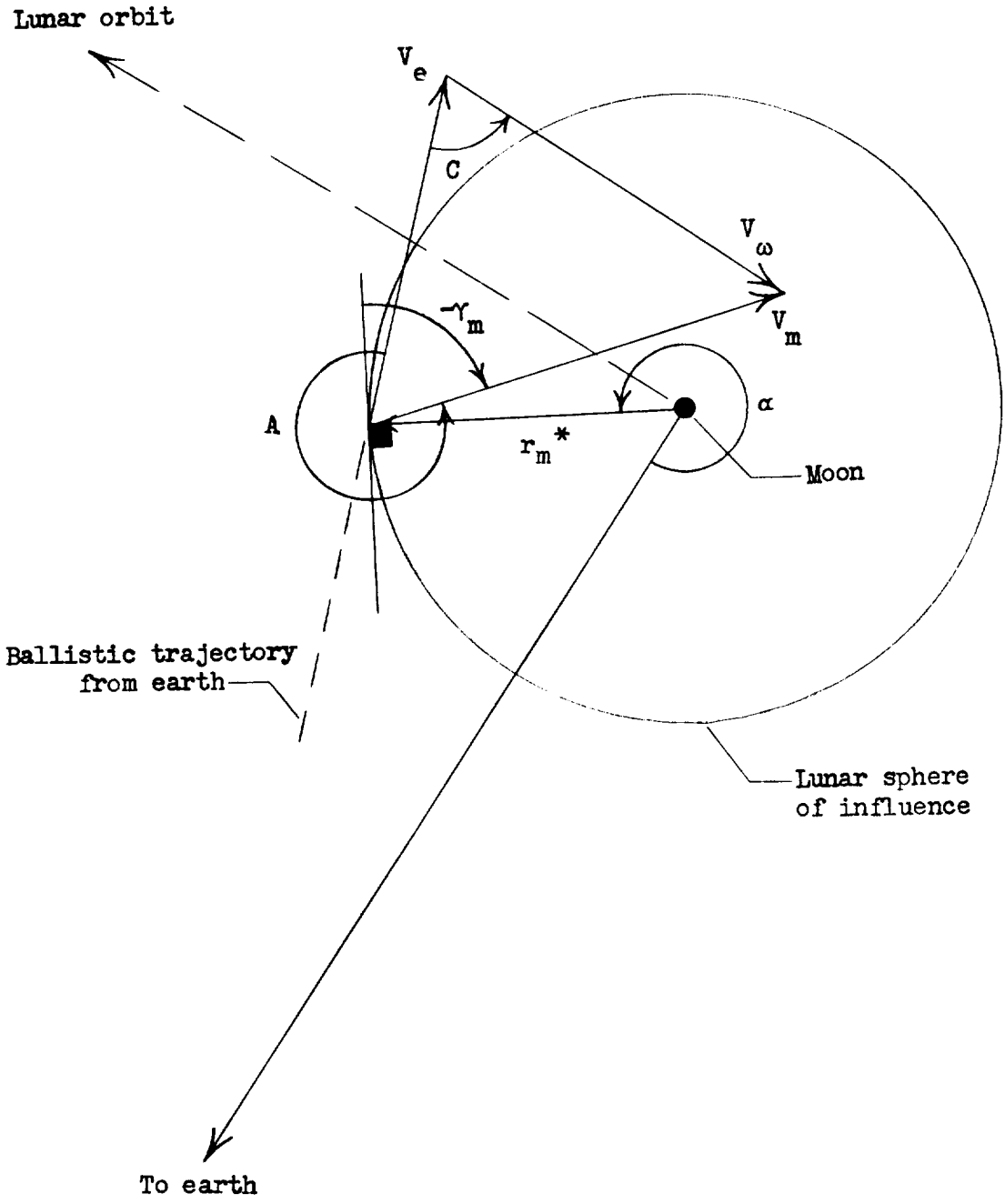

Figure 2.- Sketch showing definition of parameters at time of vehicle entry into lunar sphere of influence. Positive directions shown unless otherwise indicated.

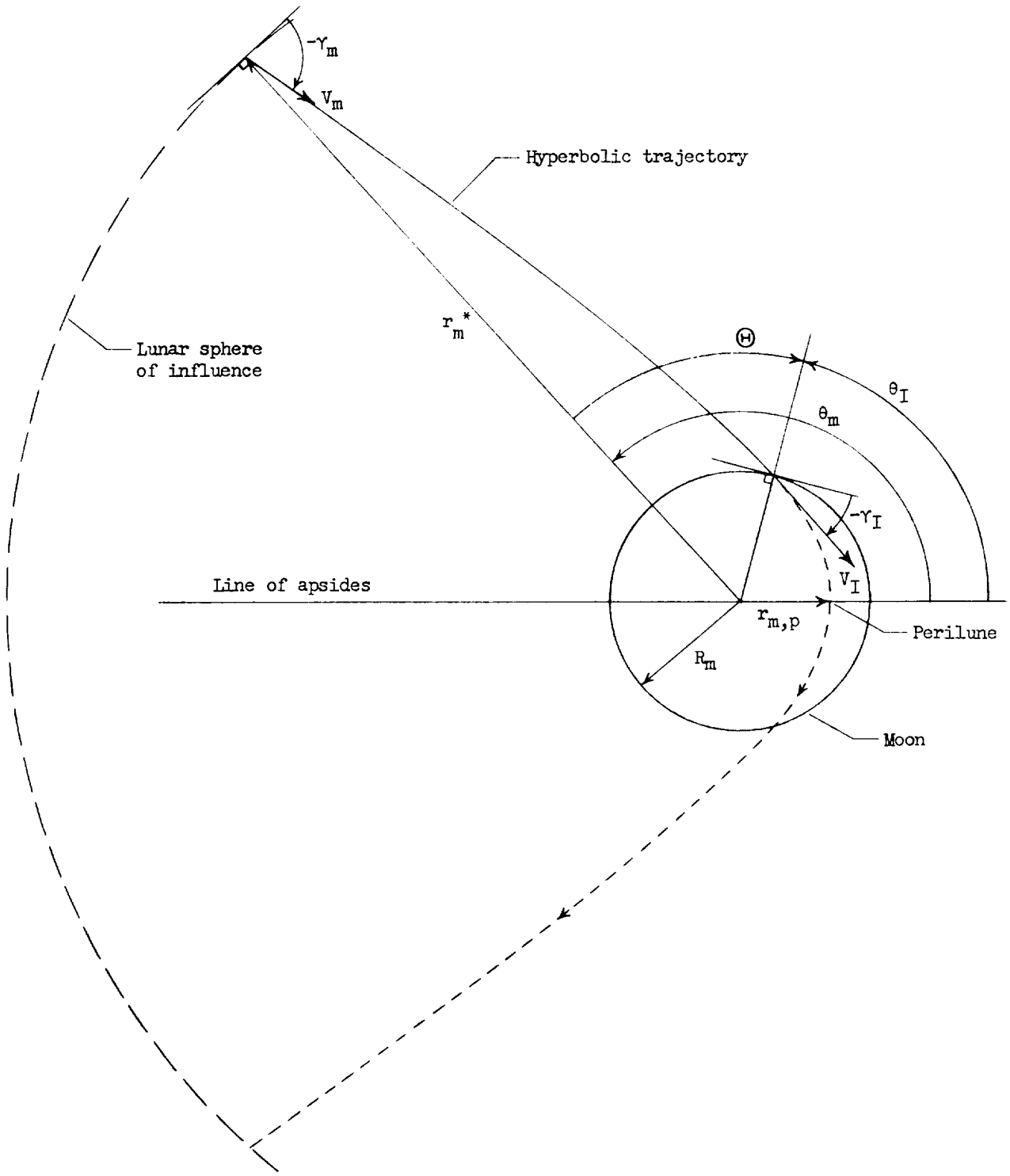

Figure 5.- Sketch showing definition of parameters for hyperbolic-impact trajectory within the lunar sphere of influence. Positive directions shown unless otherwise indicated.

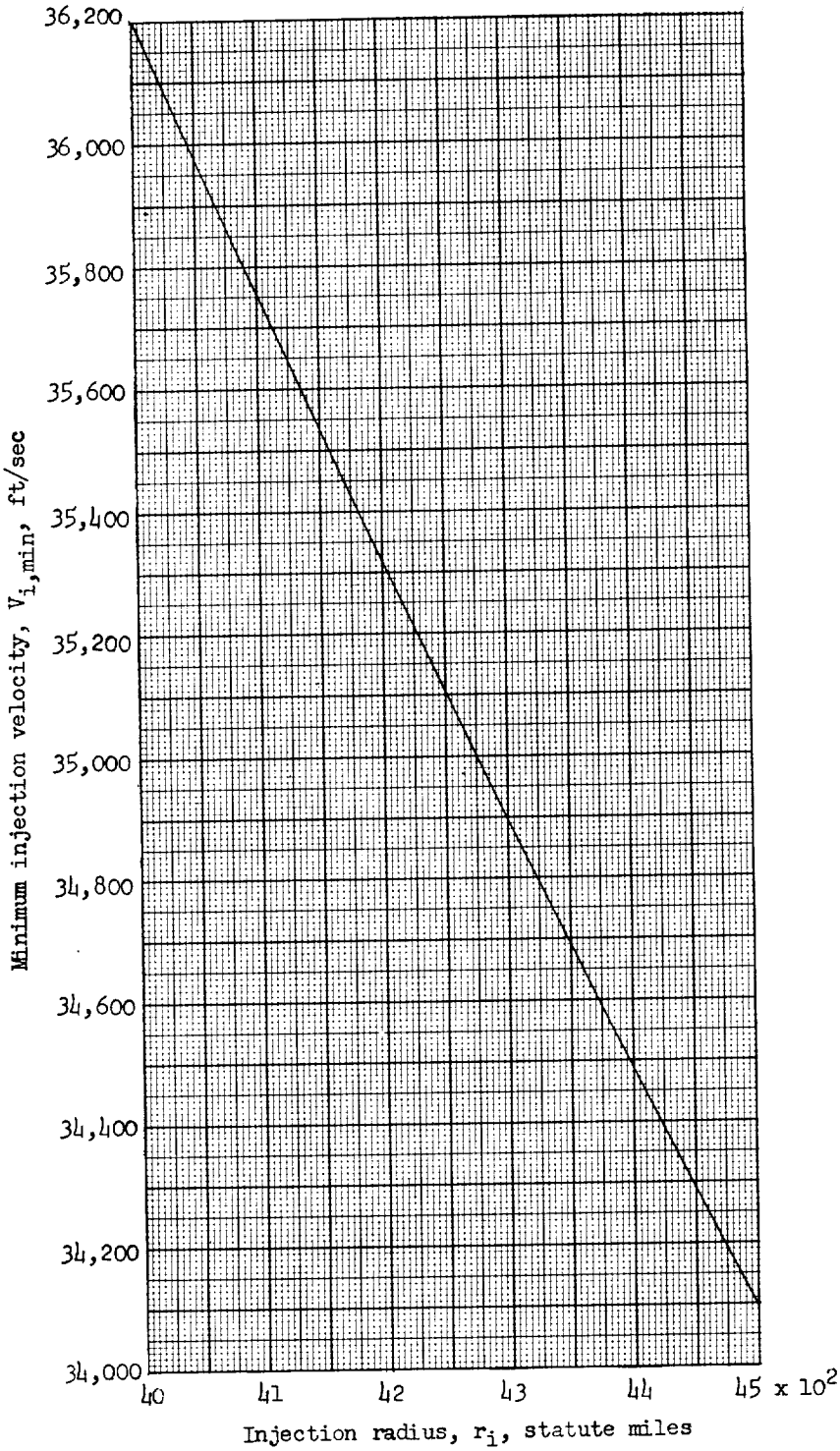

Figure 4.- Minimum injection velocity to reach the moon. Injection flight-path angle $\gamma_i = 0^\circ$ to 60°.

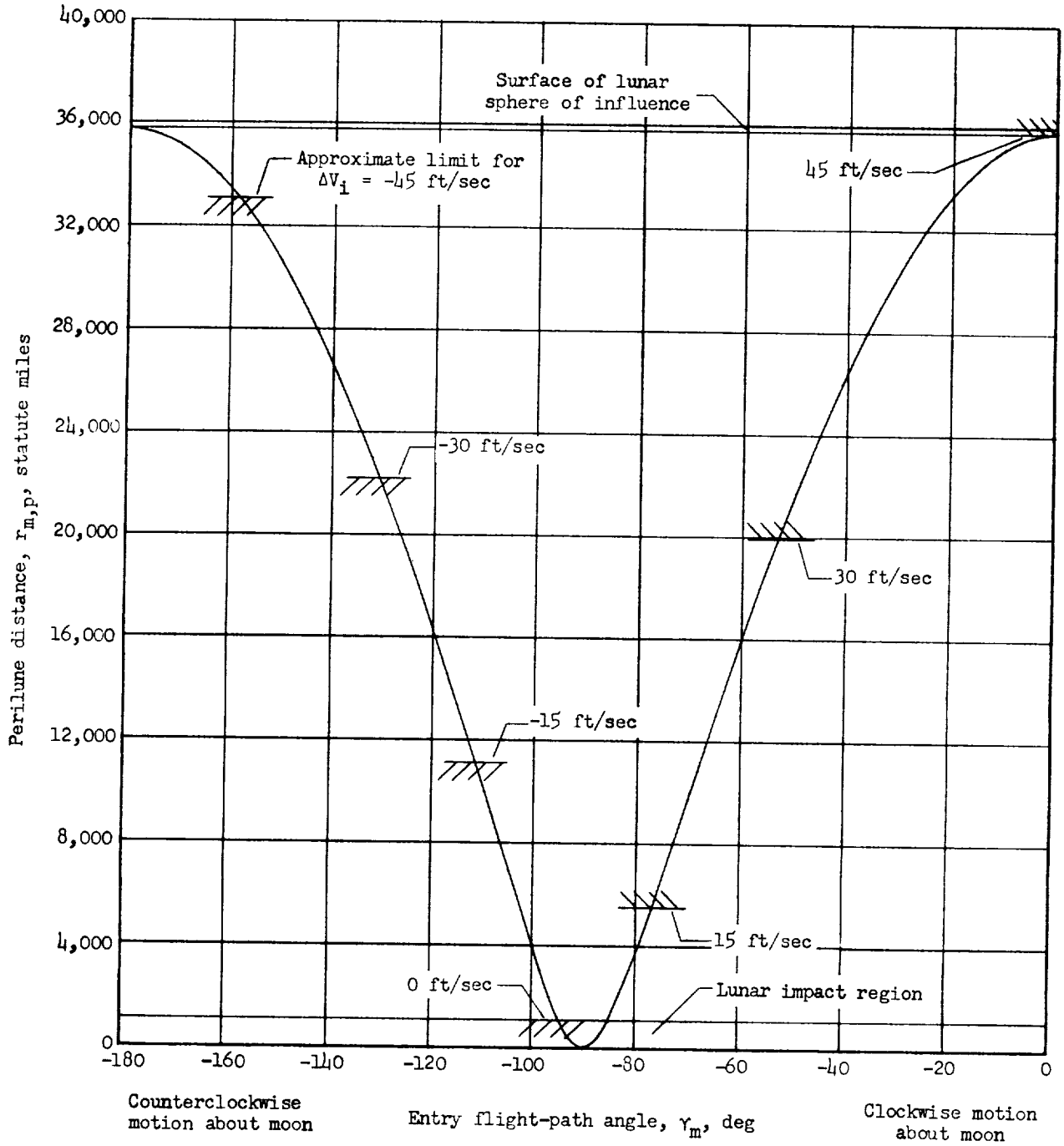

(a) $\Delta V_i < 45$ ft/sec.

Figure 5.- Variation of entry flight-path angle with perilune distance for ascending trajectories and for descending trajectories (up to ΔV_i = 162 ft/sec). Data apply for all injection flight-path angles and all injection altitudes.

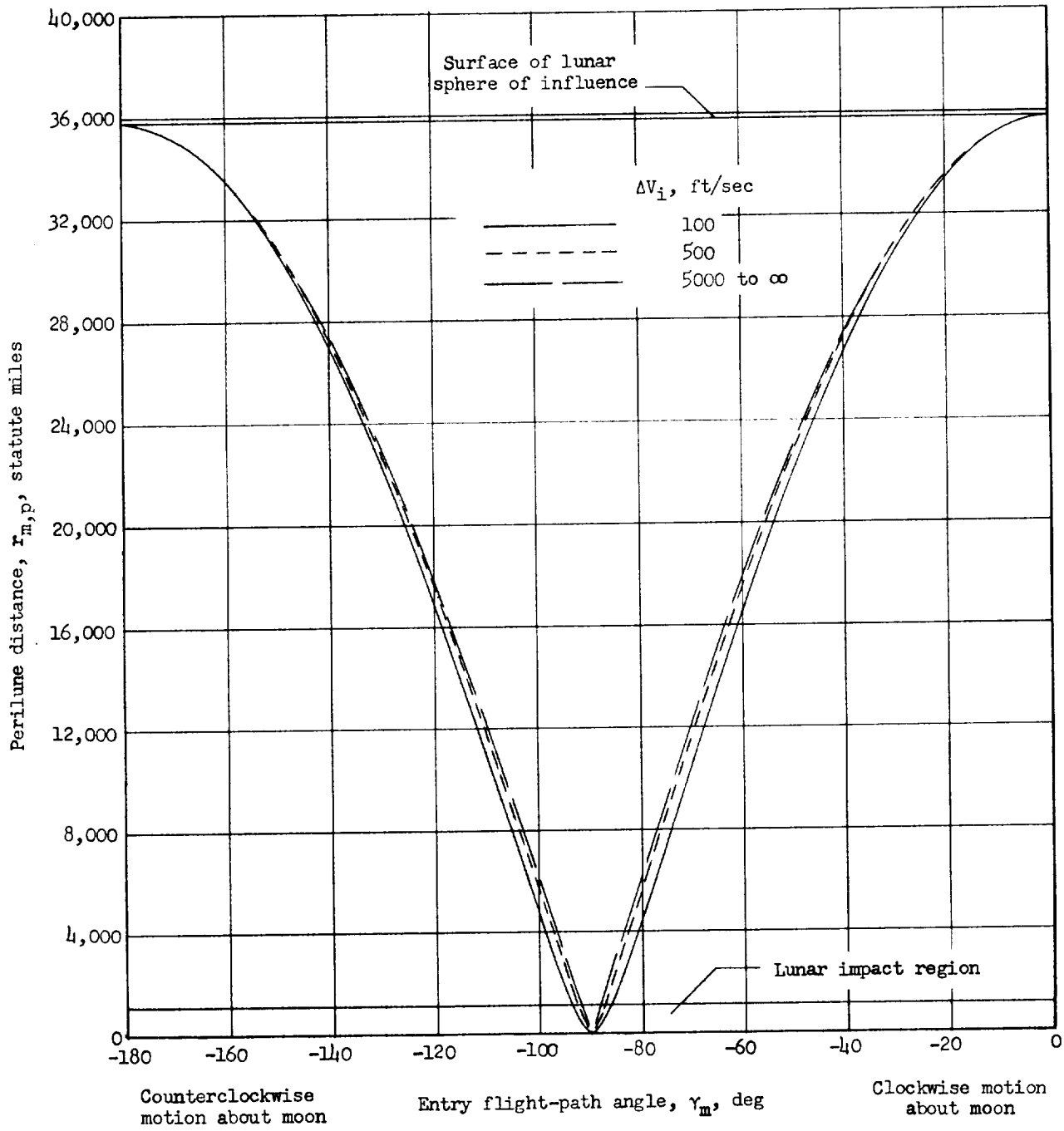

(b) $\Delta V_i > 45$ ft/sec.

Figure 5.- Concluded.

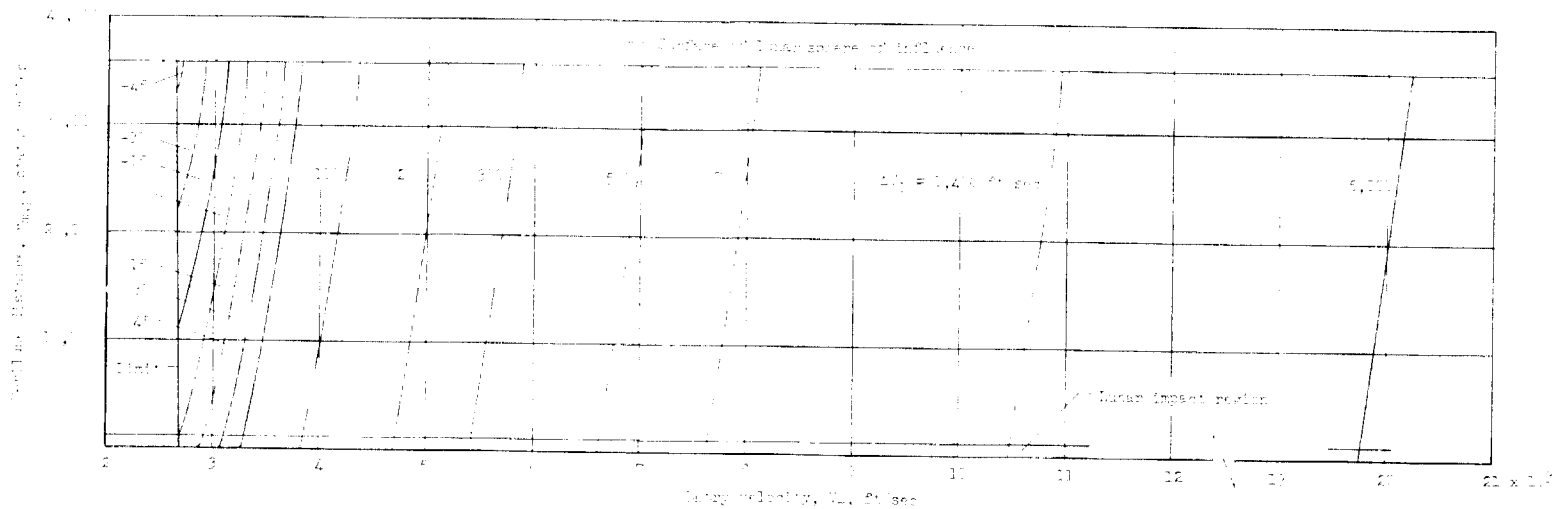

(a) $\gamma_i = 0^\circ$; counterclockwise motion about moon.

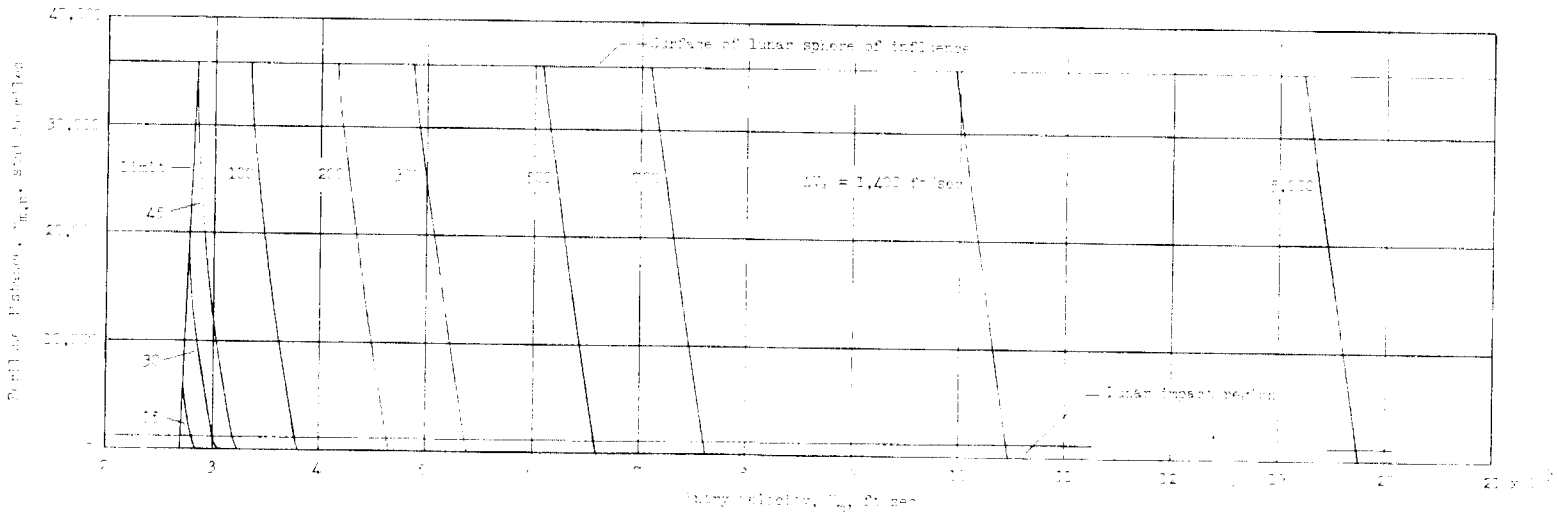

(b) $\gamma_i = 0^\circ$; clockwise motion about moon.

Figure 6.- Variation of entry velocity with perilune distance for ascending trajectories. Data apply for injection radii at or near 4,100 statute miles (altitudes near 140 miles).

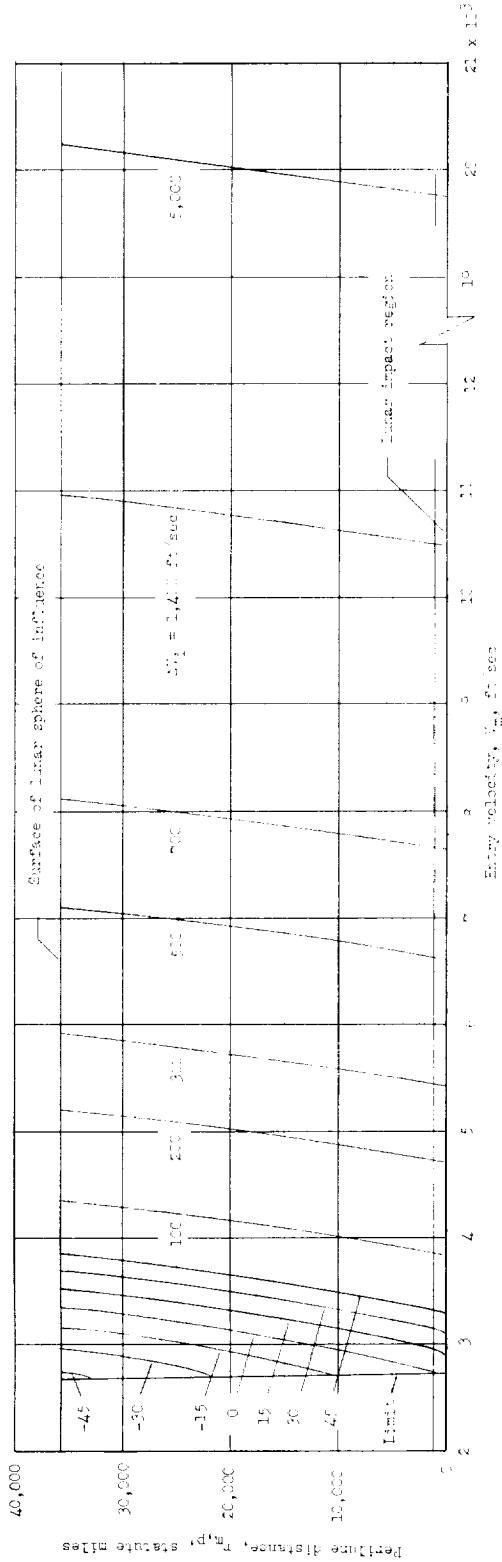

(c) $\gamma_1 = 20^\circ$; counterclockwise motion about moon.

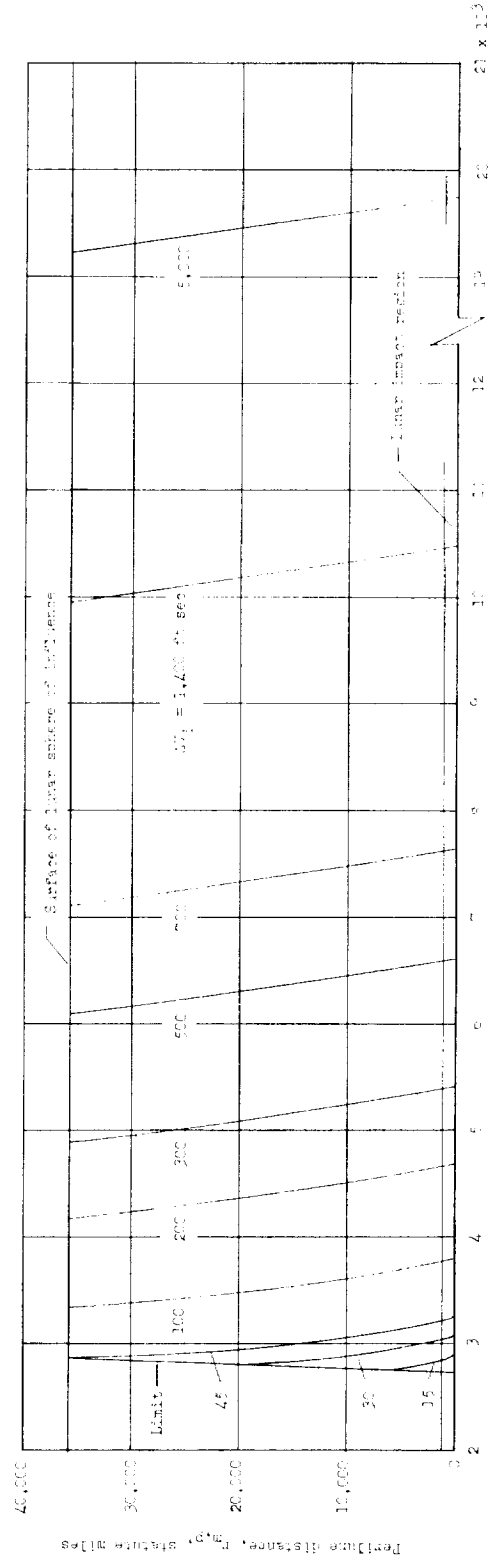

(d) $\gamma_1 = 20^\circ$; clockwise motion about moon.

Figure 6.- Continued.

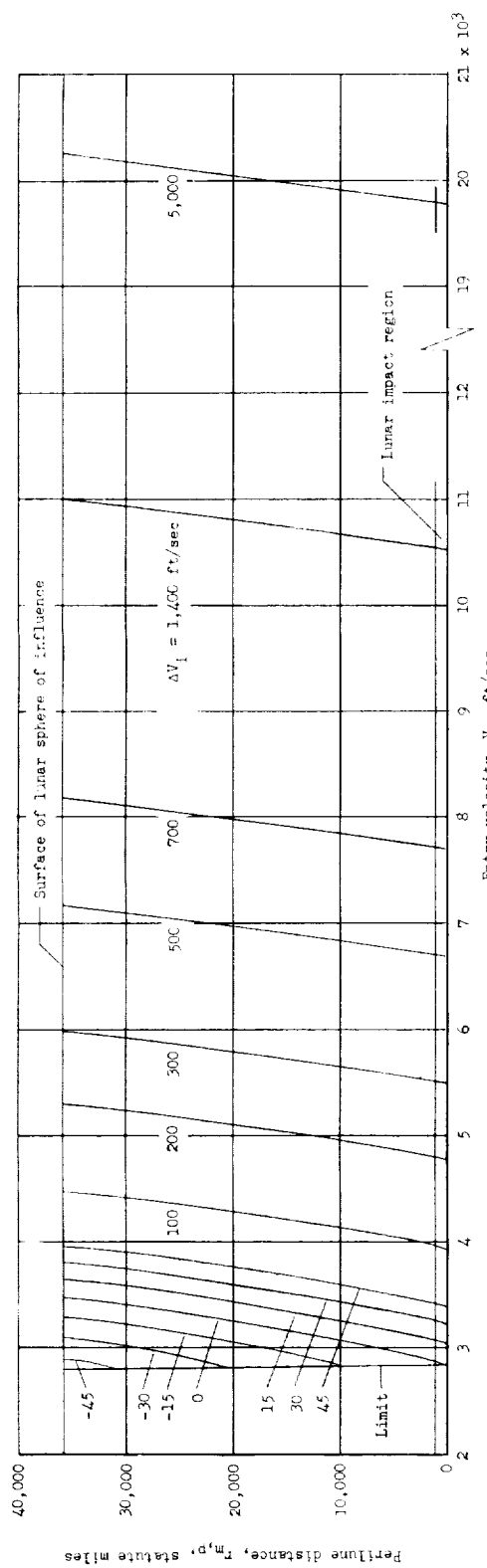

(e) γ_i = 40°; counterclockwise motion about moon.

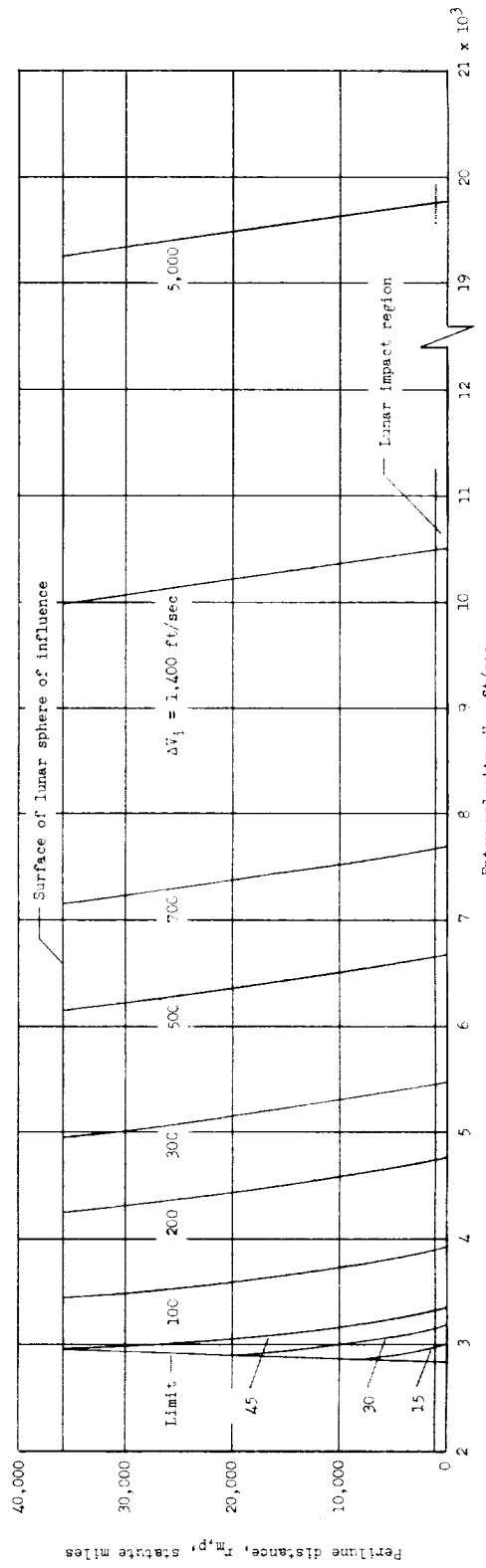

(f) γ_i = 40°; clockwise motion about moon.

Figure 6.- Continued.

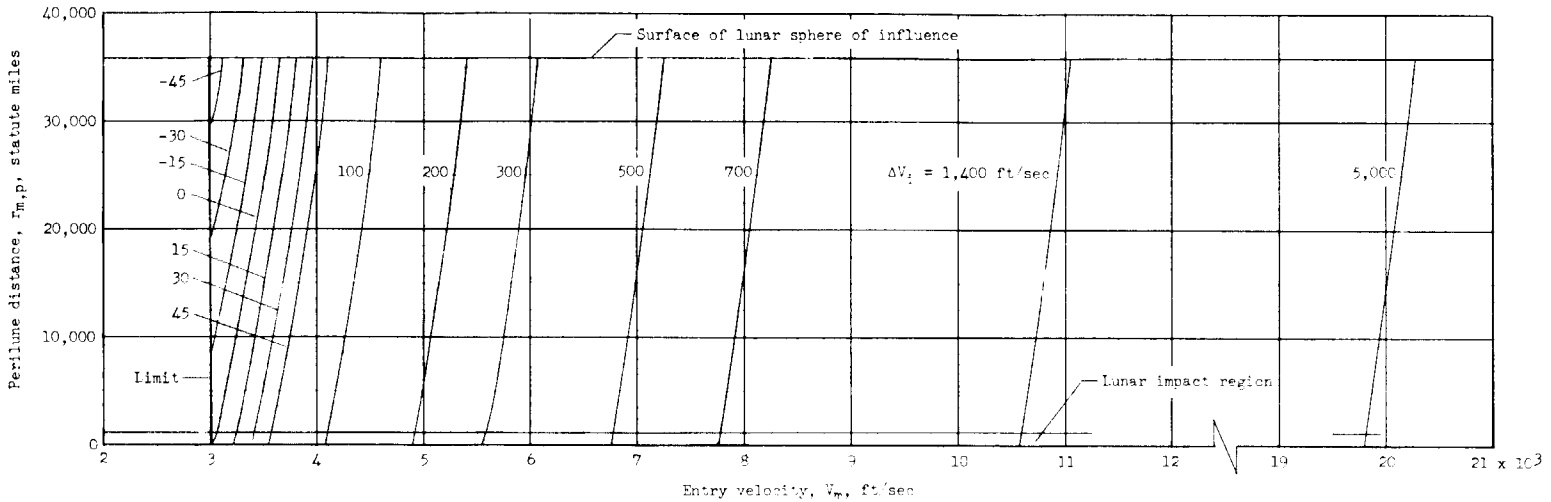

(g) $\gamma_i = 60^\circ$; counterclockwise motion about moon.

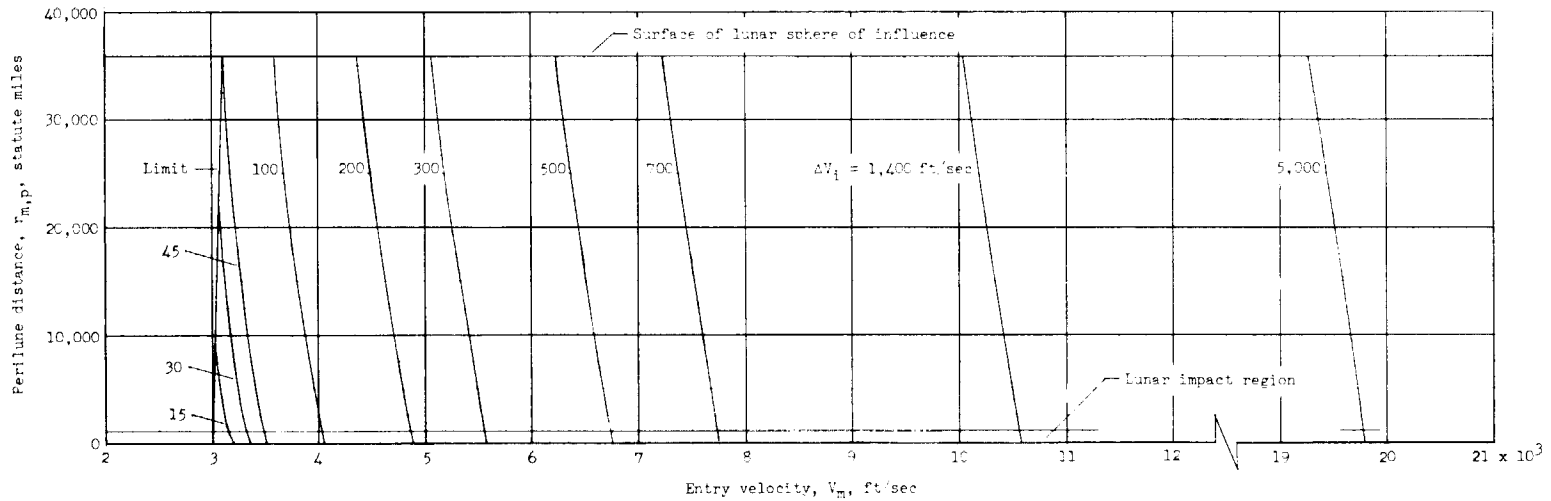

(h) $\gamma_i = 60^\circ$; clockwise motion about moon.

Figure 6.- Concluded.

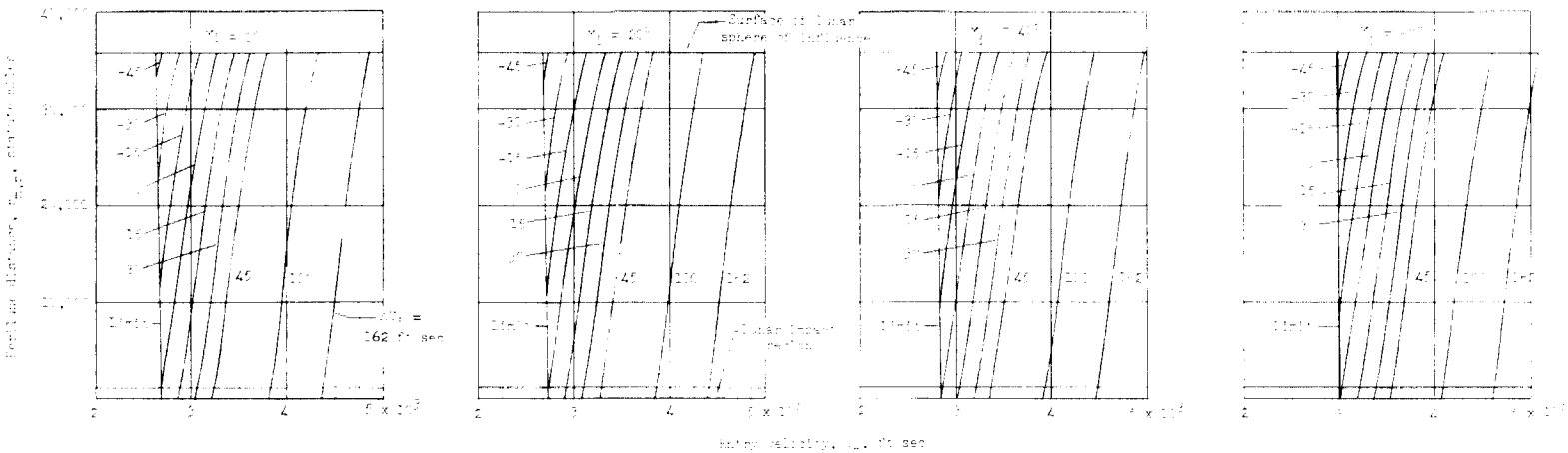

(a) Counterclockwise motion about moon.

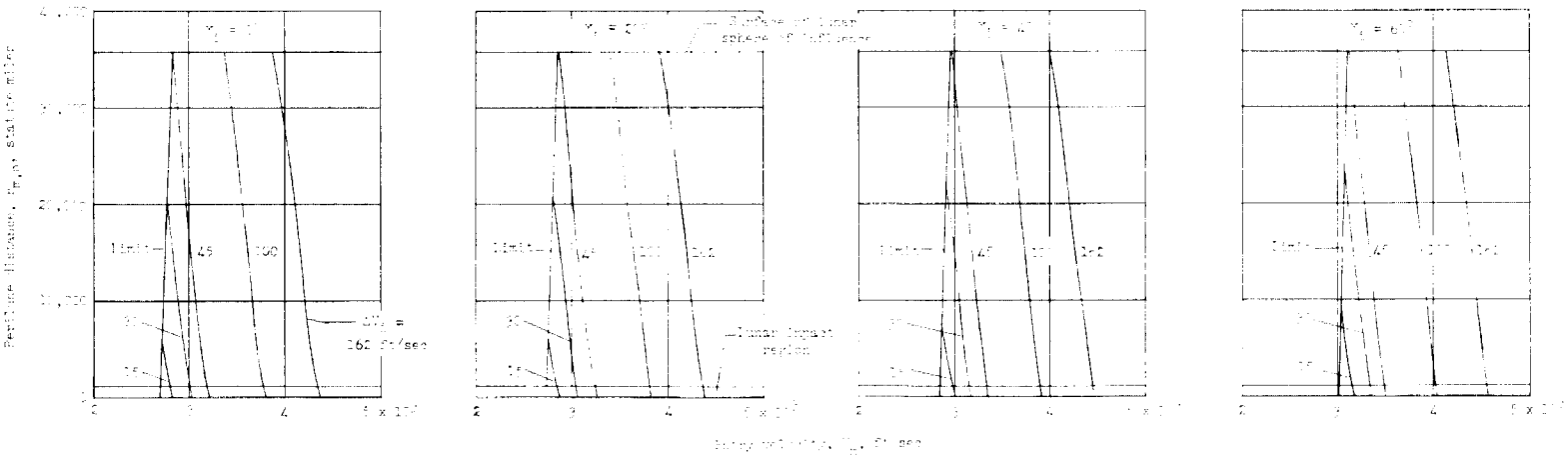

(b) Clockwise motion about moon.

Figure 7.- Variation of entry velocity with perilune distance for descending trajectories. Data apply for injection radii at or near 4,100 statute miles (altitudes near 140 miles).

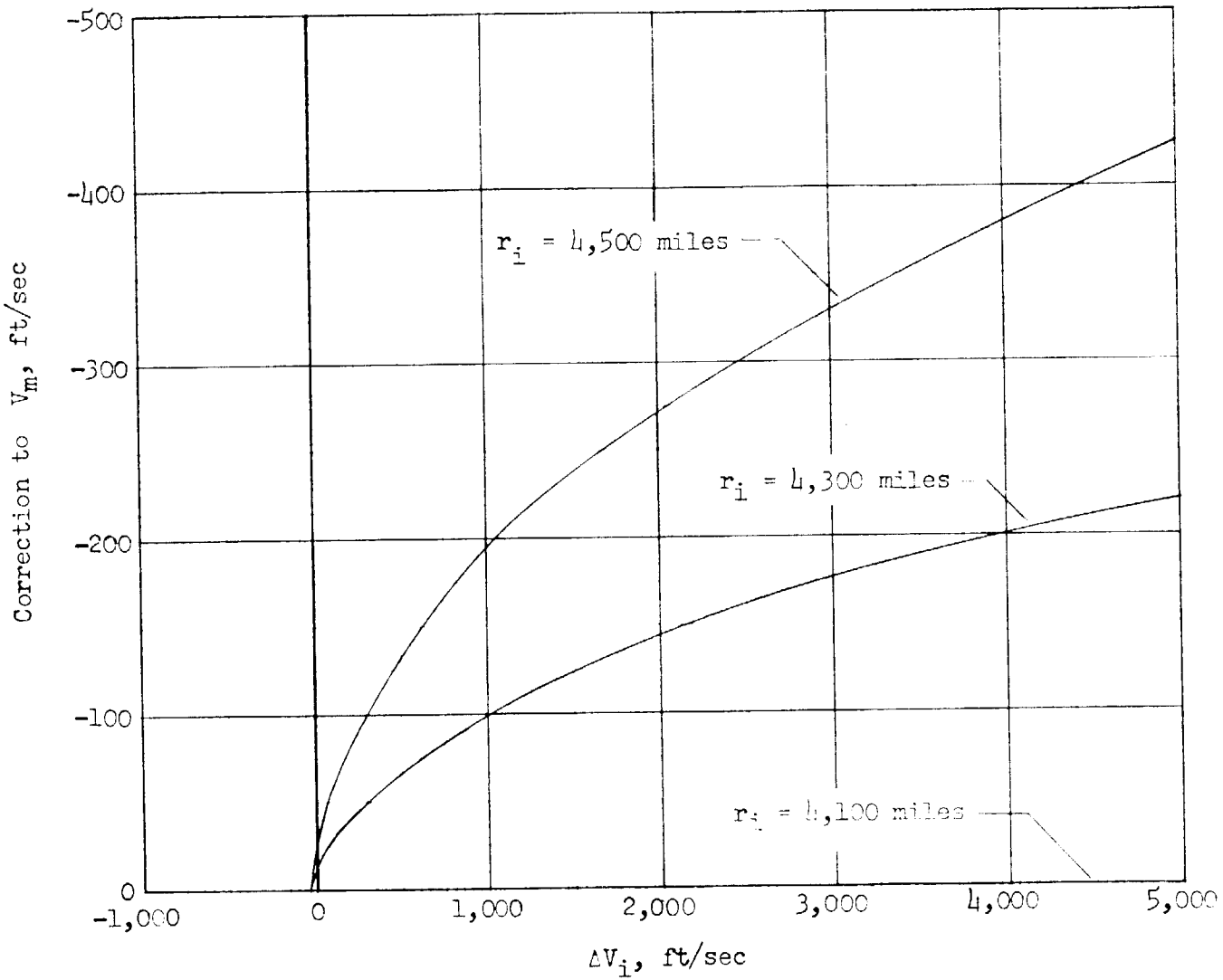

Figure 8.- Correction to entry-velocity values of figures 6 and 7 to account for effect of injection altitude.

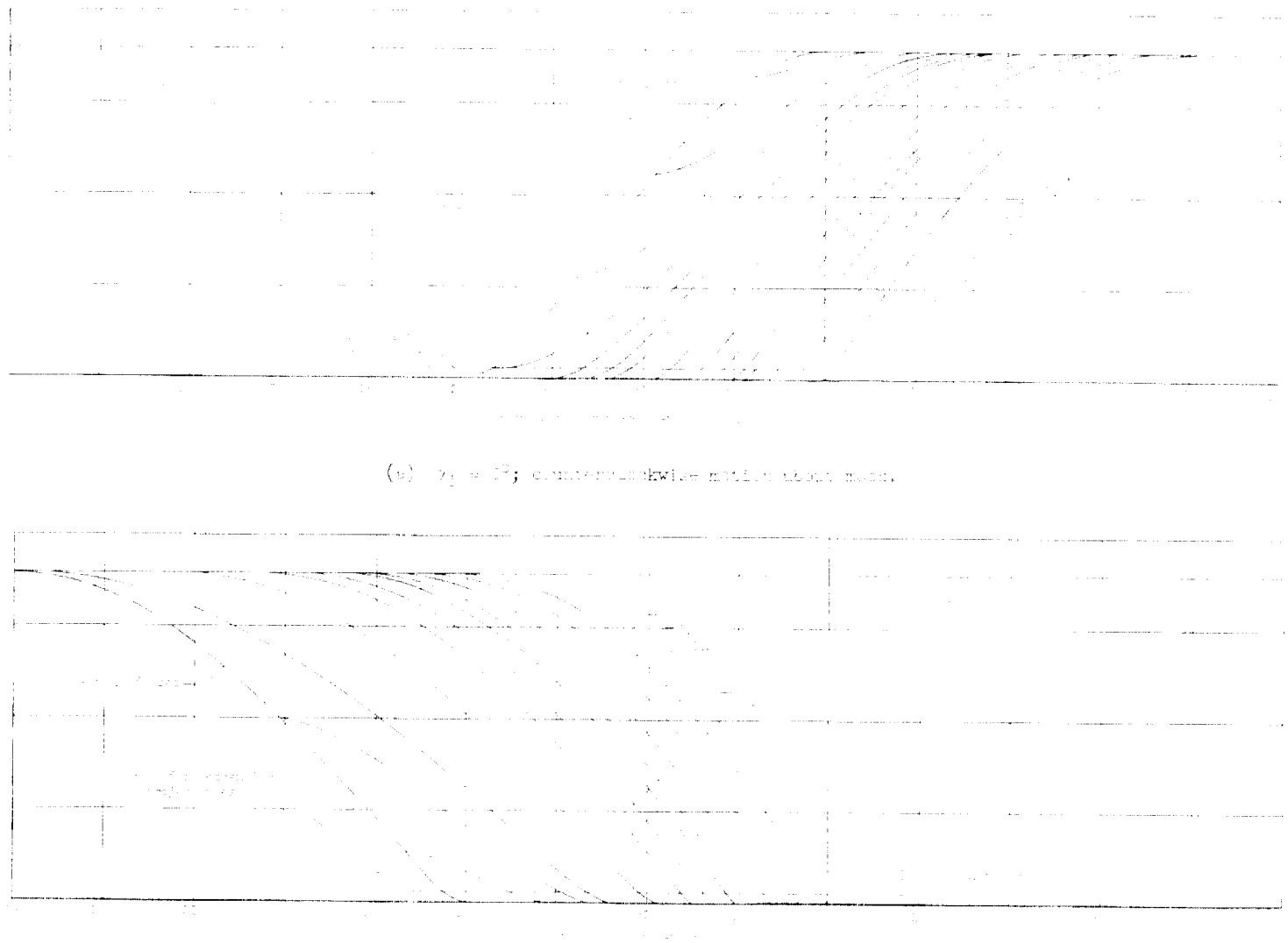

Figure 9.- Variation of entry location with perilune distance for allowable trajectories. Data apply for all injection altitudes.

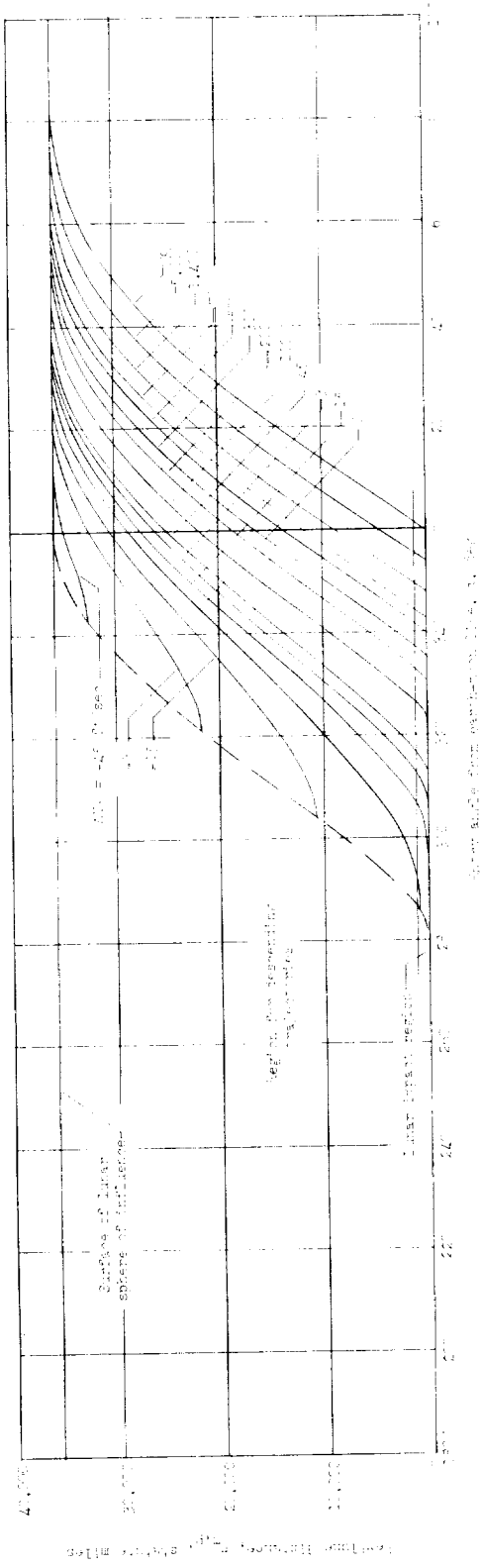

(c) $\gamma_1 = 20^\circ$; counterclockwise motion about moon.

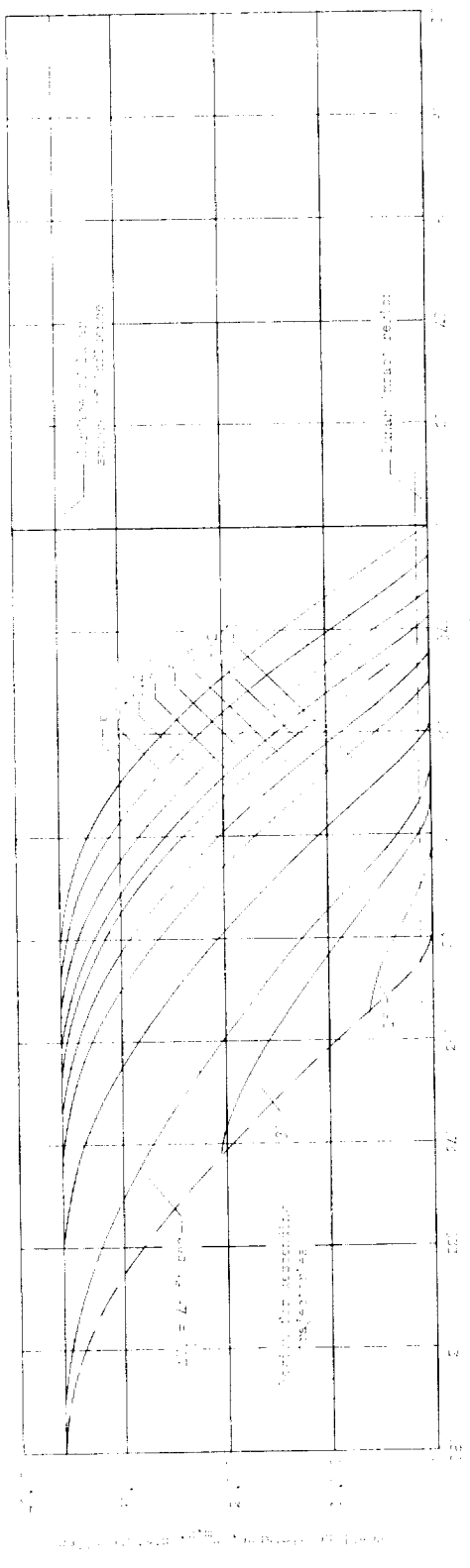

(d) $\gamma_1 = 20^\circ$; clockwise motion about moon.

Figure 9.- Continued.

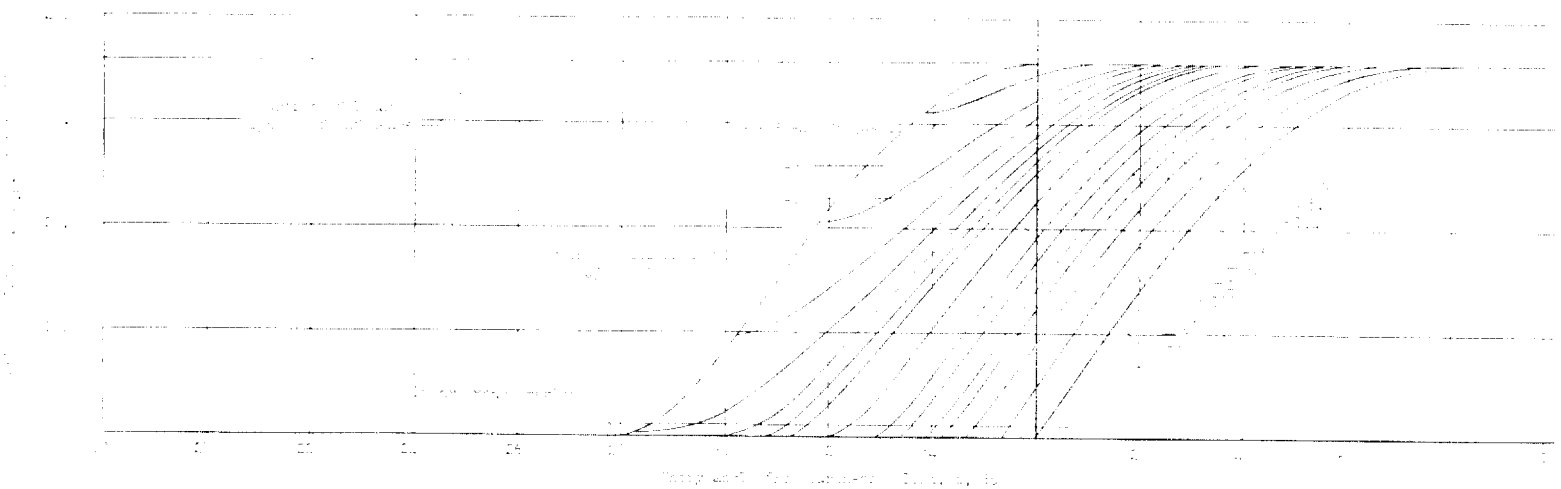

(e) $\gamma_2 = 40°$; counterclockwise motion about moon.

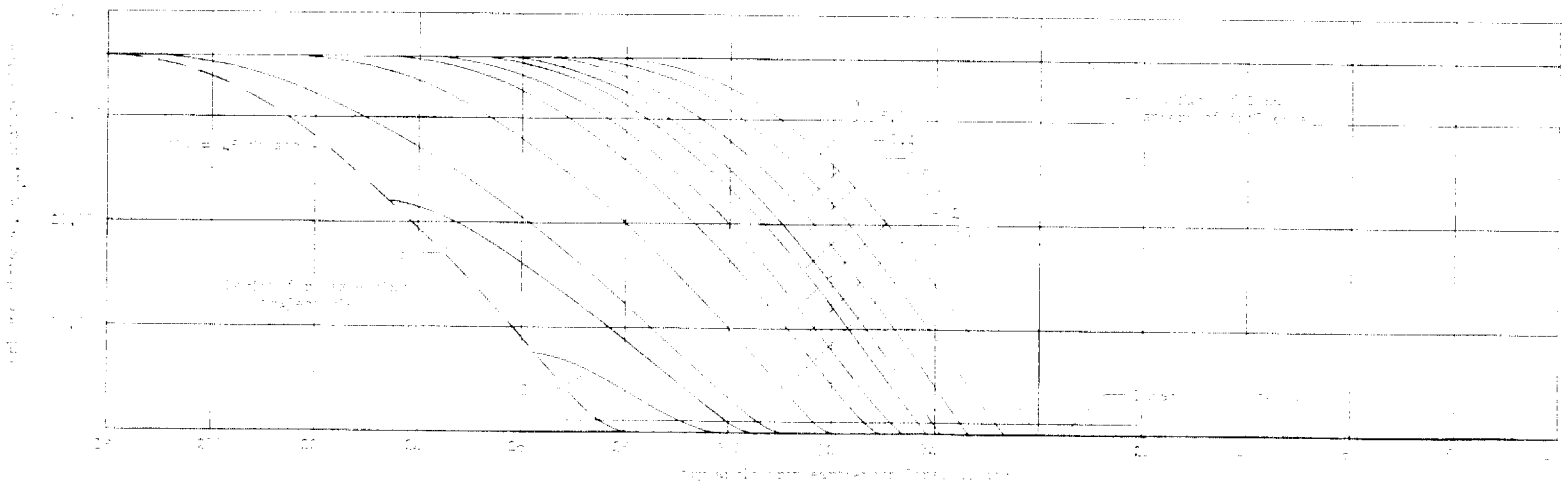

(f) $\gamma_2 = 40°$; clockwise motion about moon.

Figure 9.- Continued.

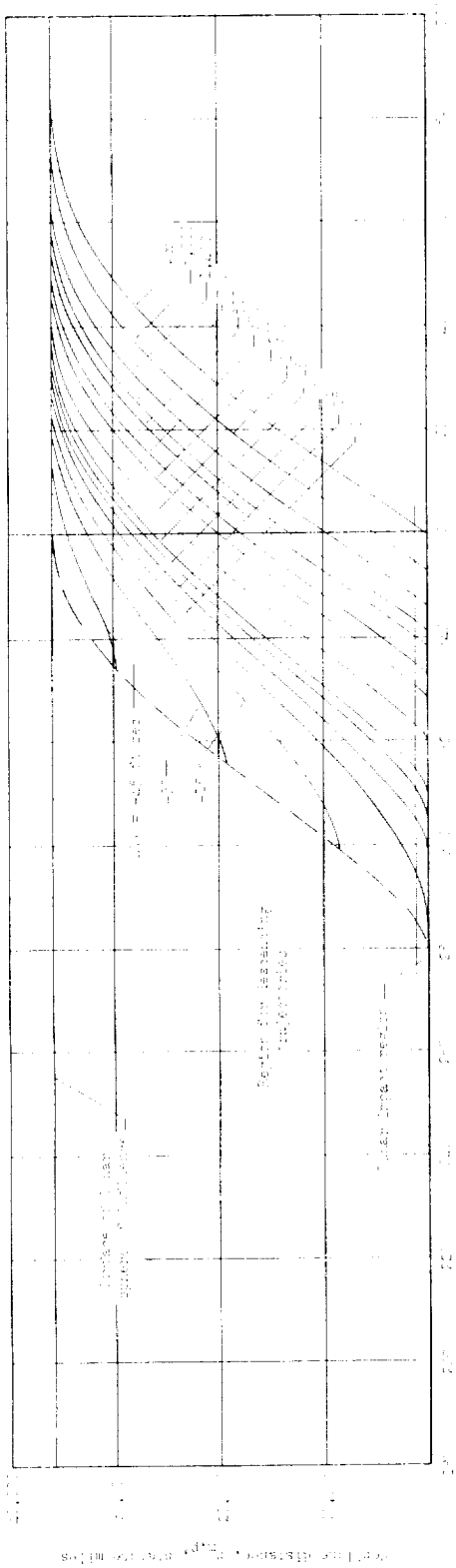

(g) $\gamma_1 = 60°$; counterclockwise motion about moon.

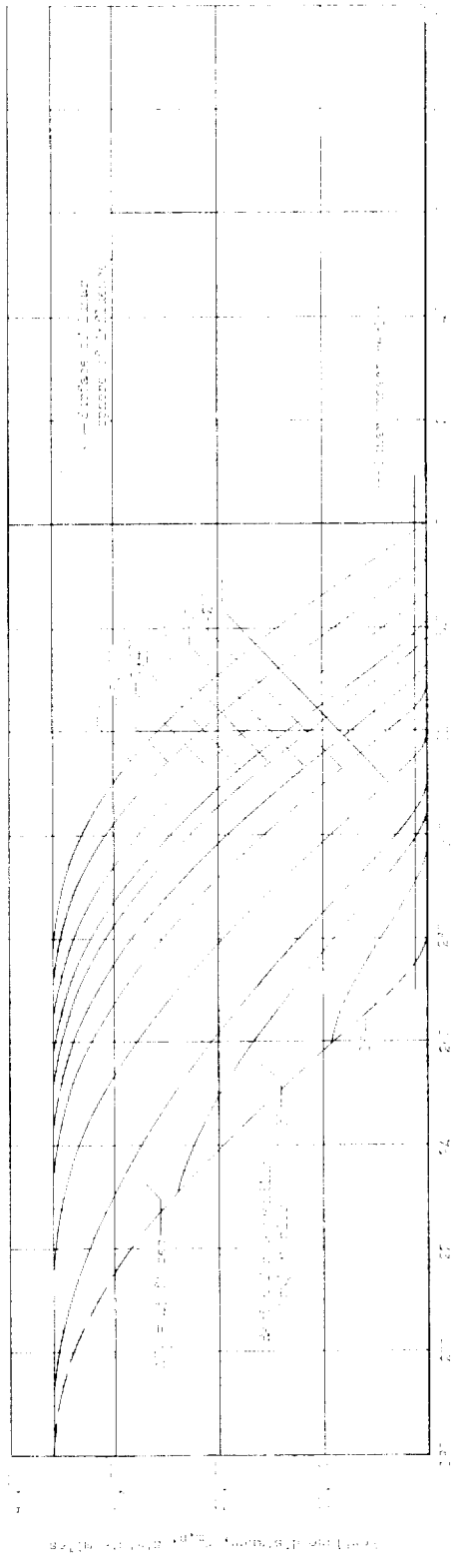

(h) $\gamma_1 = 60°$; clockwise motion about moon.

Figure 9.- Concluded.

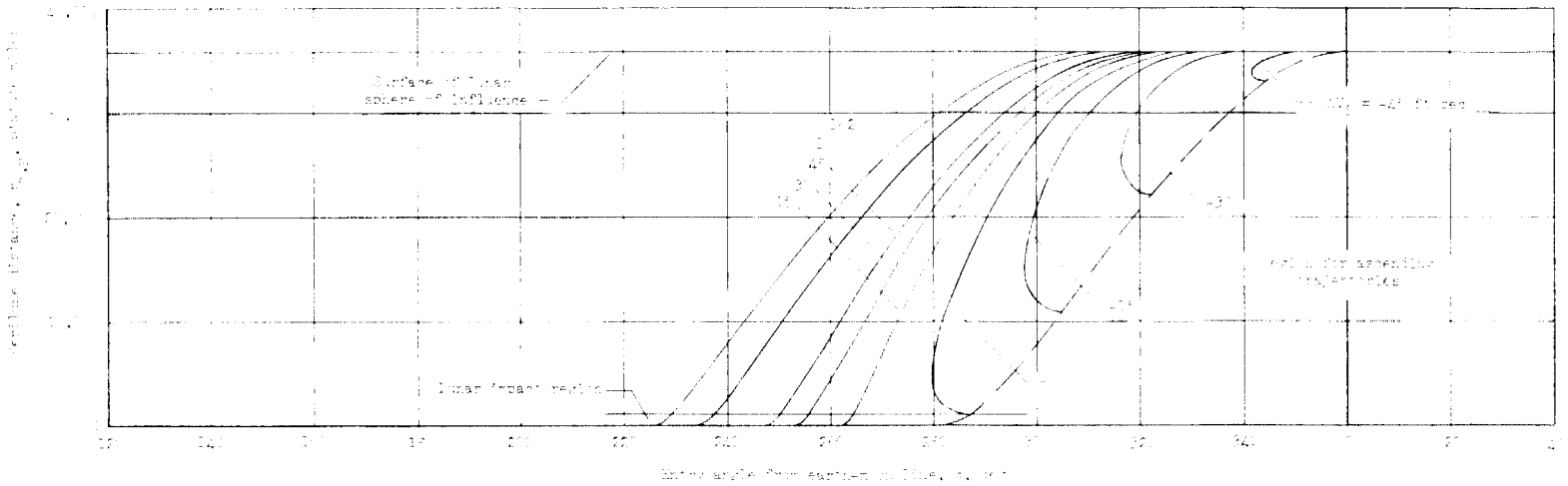

(a) $\gamma_i = 0^\circ$; counterclockwise motion about moon.

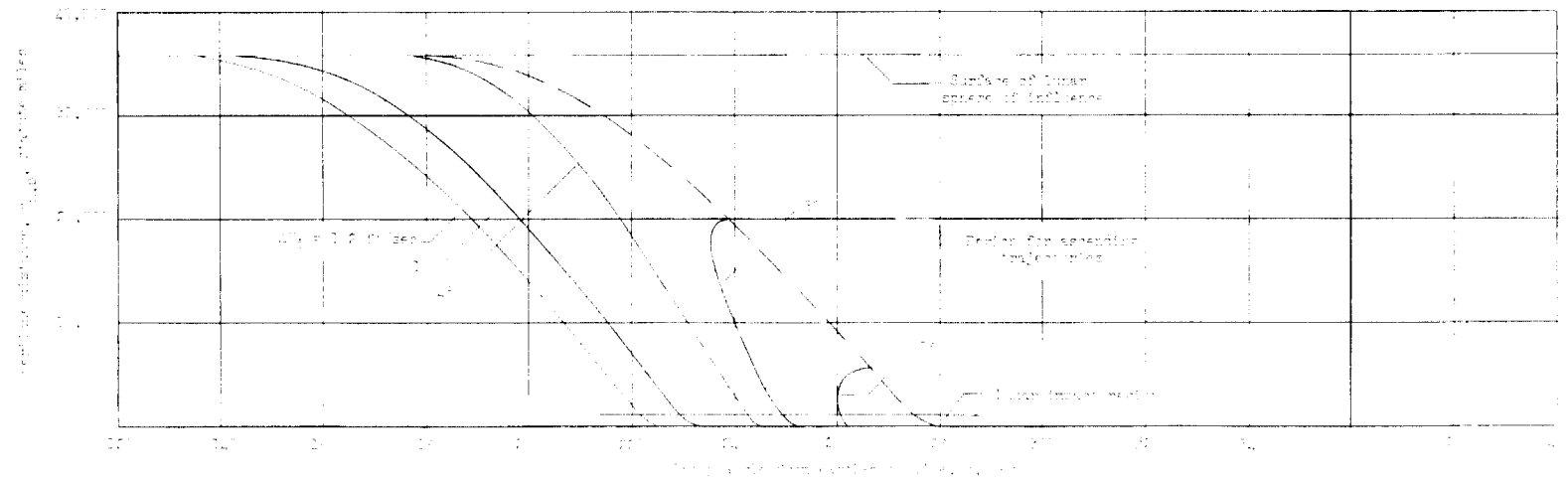

(b) $\gamma_i = 0^\circ$; clockwise motion about moon.

Figure 10.- Variation of entry location with perilune distance for descending trajectories. Data apply for all injection altitudes.

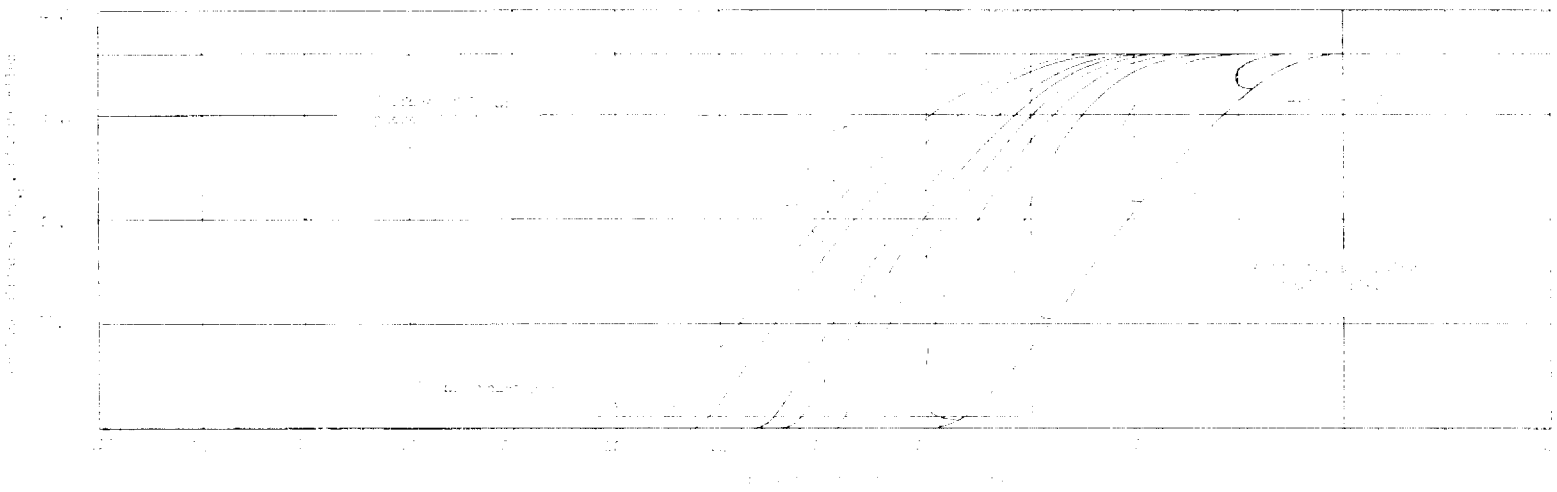

(c) [illegible]

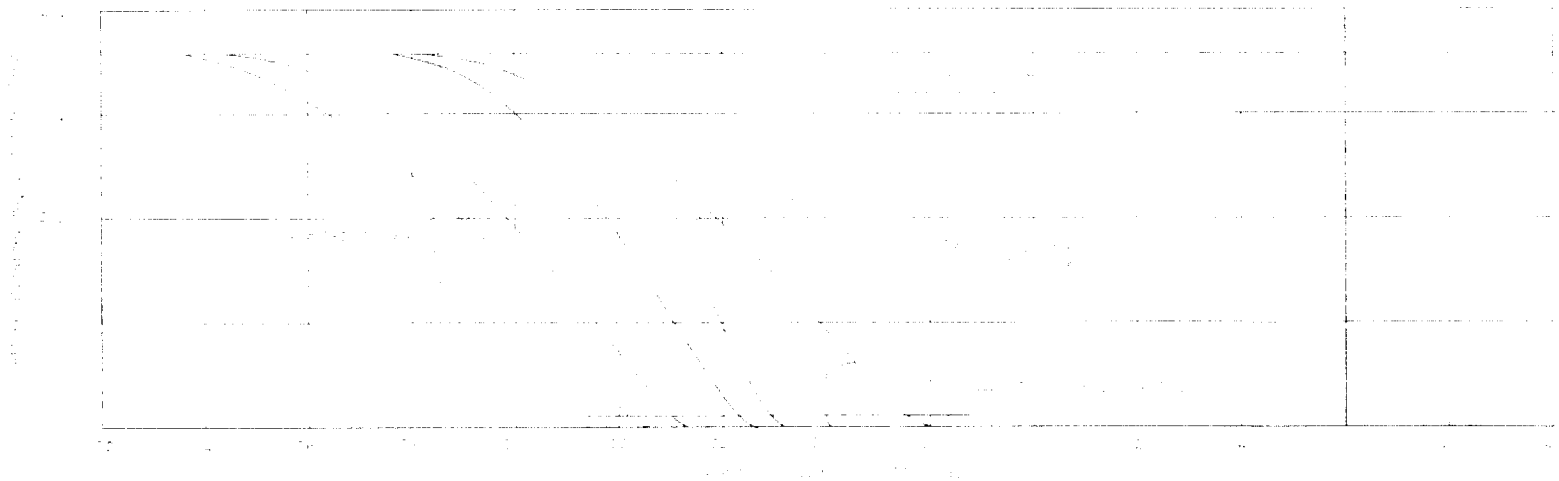

(d) [illegible]

Figure 15.- Continued.

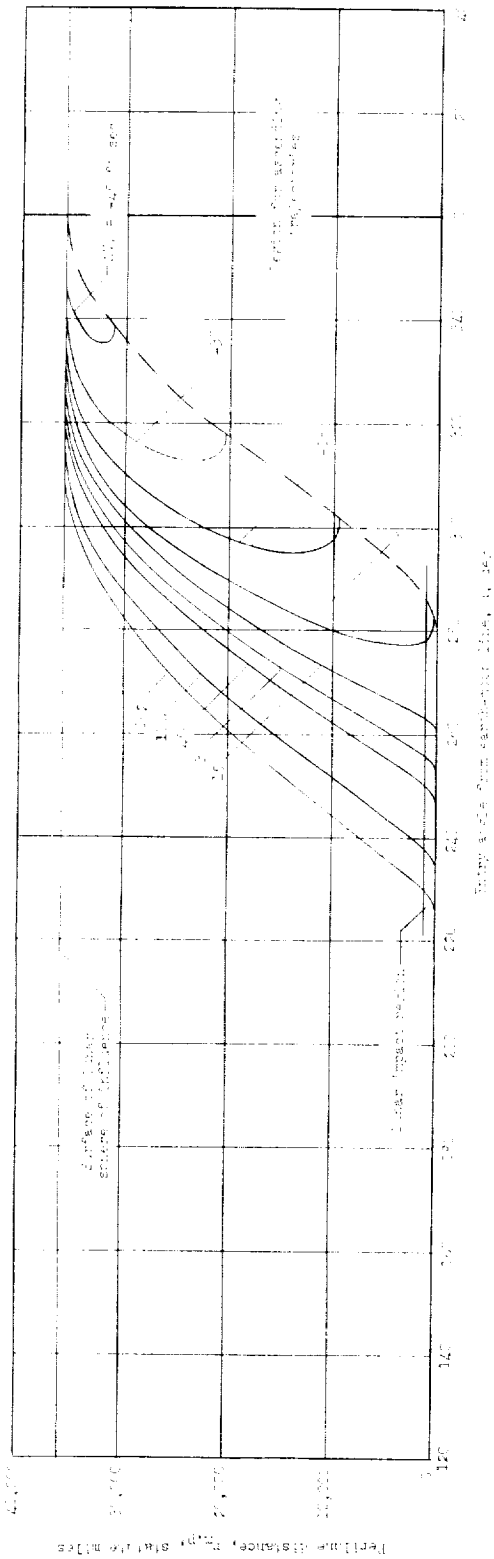

(e) $\gamma_i = 40^0$; counterclockwise motion about moon.

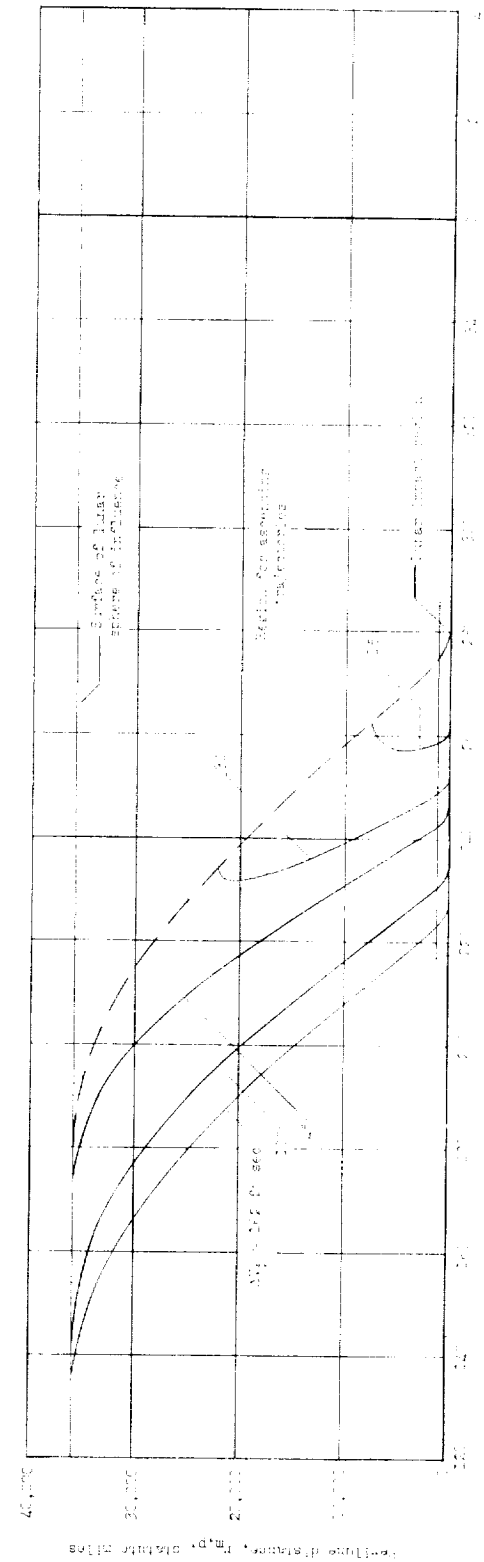

(f) $\gamma_i = 40^0$; clockwise motion about moon.

Figure 10.- Continued.

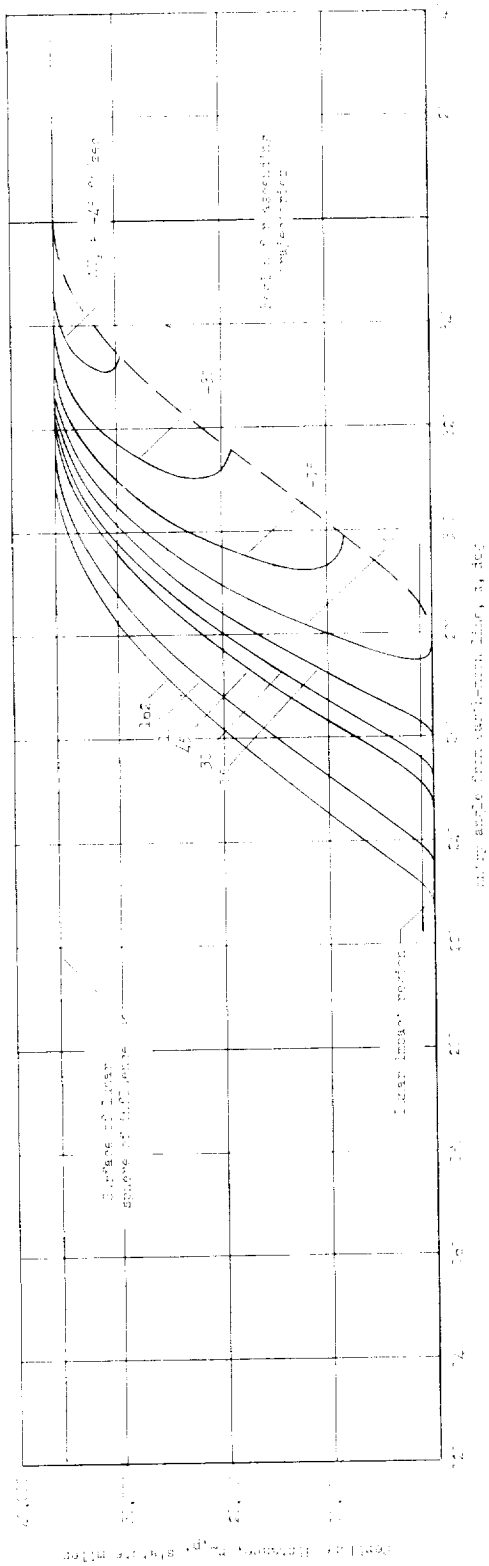

(g) $\gamma_1 = 60^\circ$; counterclockwise motion about moon.

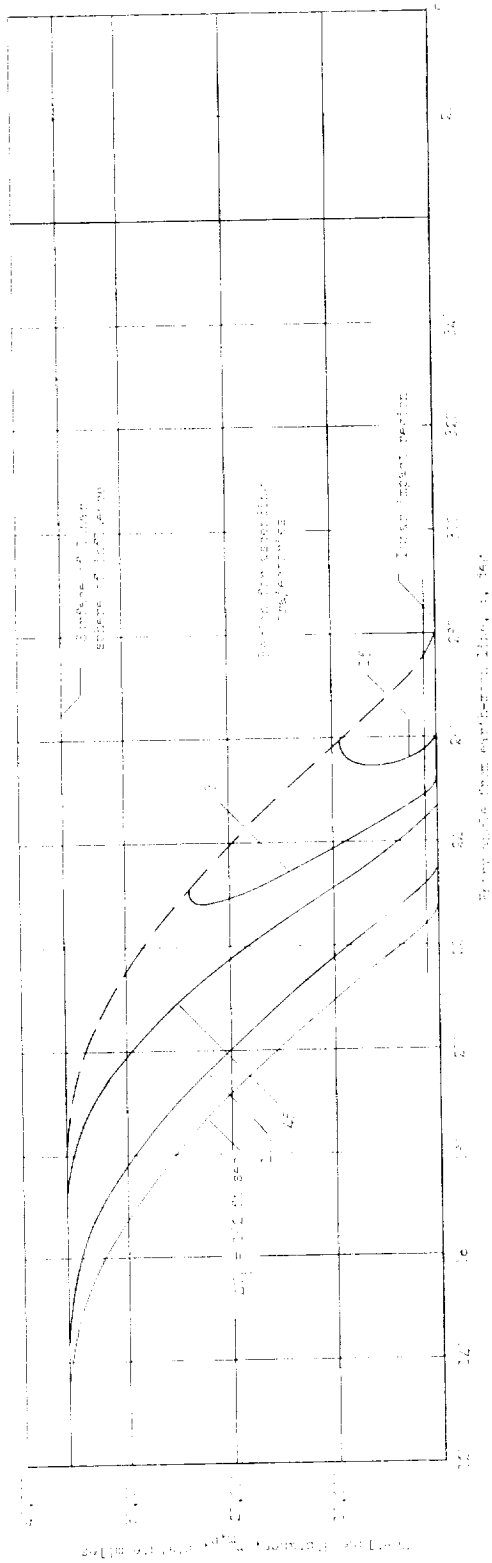

(h) $\gamma_1 = 60^\circ$; clockwise motion about moon.

Figure 10.- Concluded.

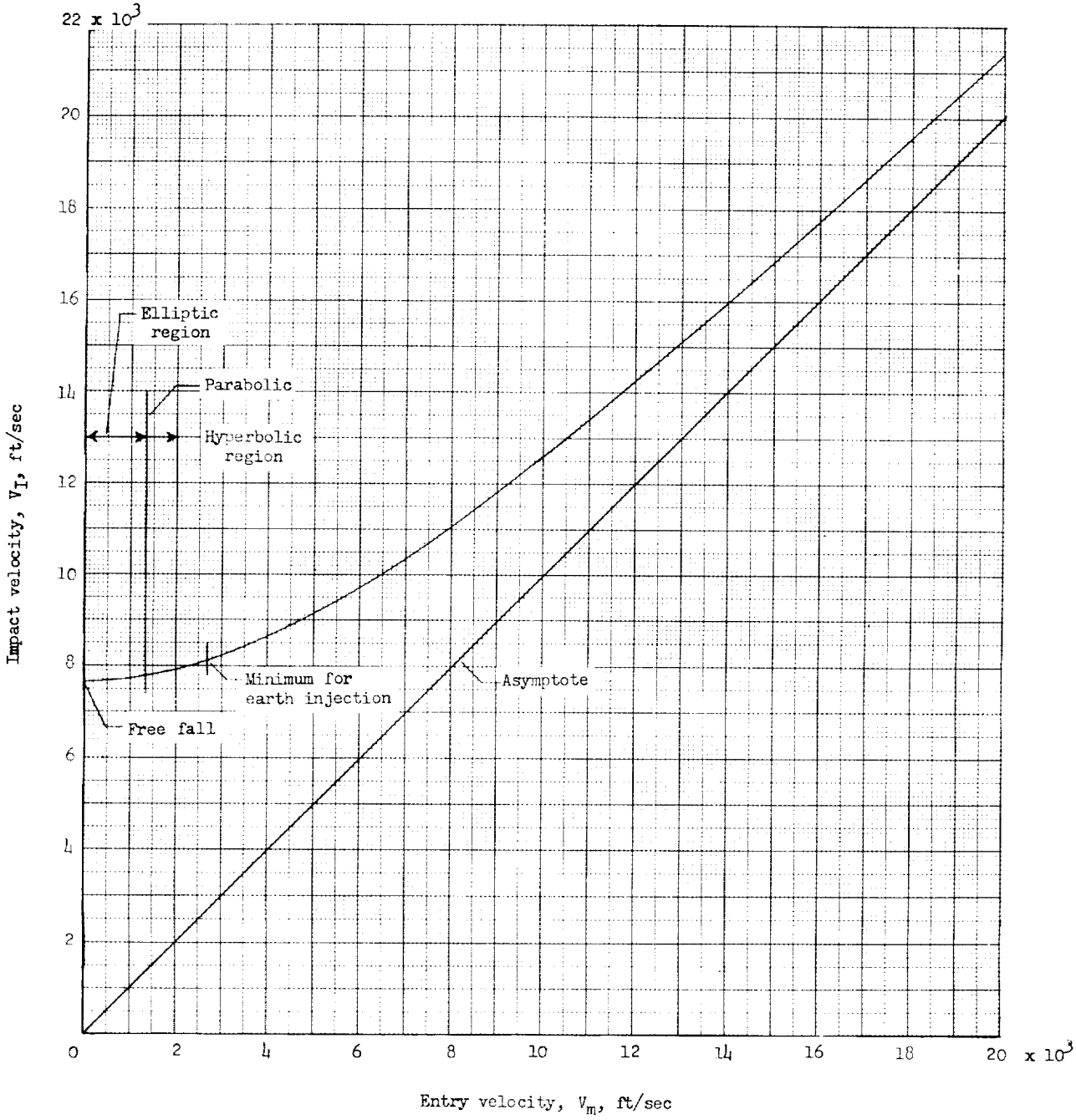

Figure 11.- Variation of impact velocity with entry velocity.

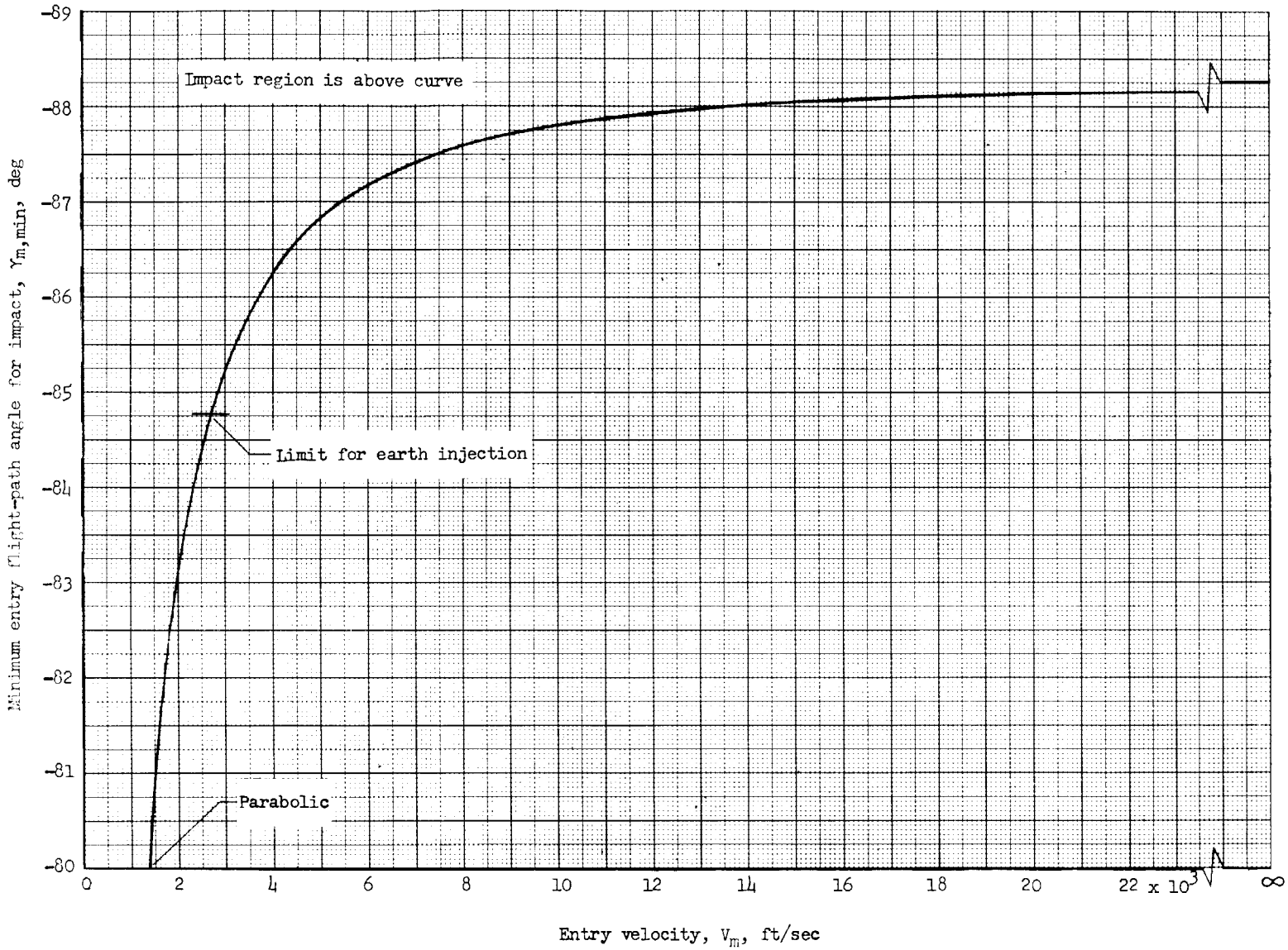

Figure 12.- Tangential impact boundary. $\gamma_{m,min} = \cos^{-1}\left(\frac{R_m V_I}{r_m^* V_m}\right)$.

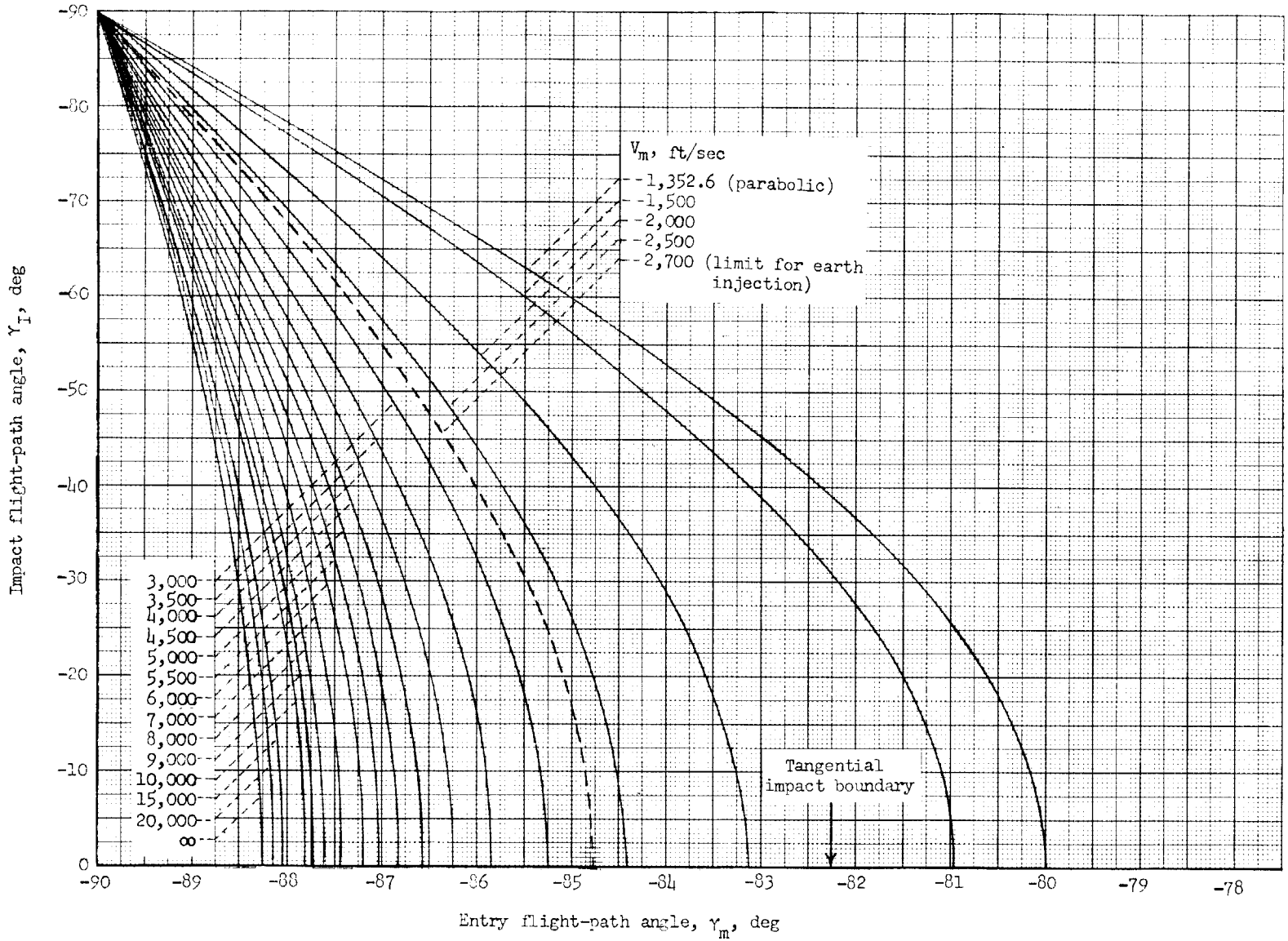

Figure 13.- Variation of impact flight-path angle with entry flight-path angle and entry velocity.

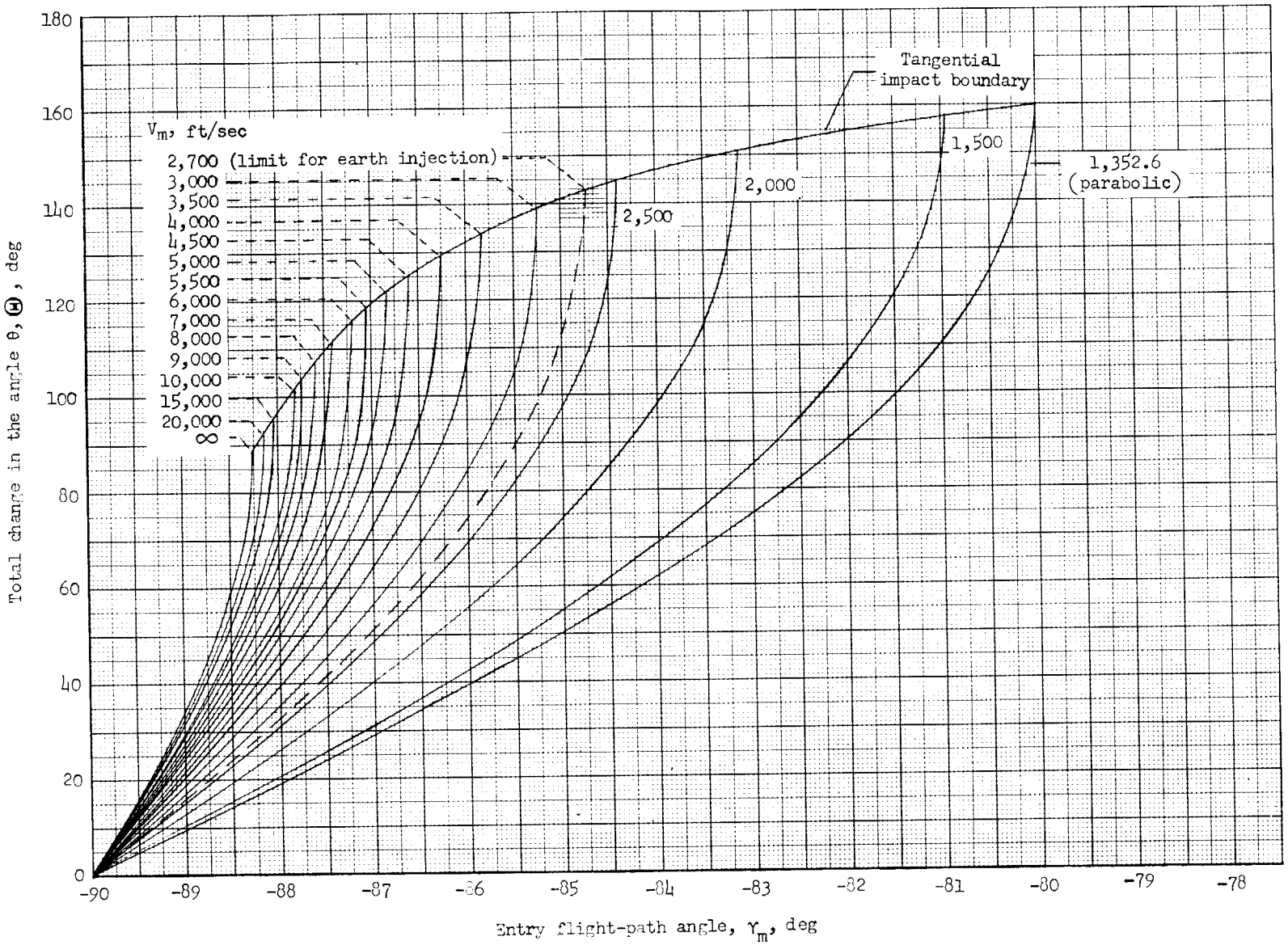

Figure 14.- Variation of total angular travel about the moon (from entry to impact) with entry flight-path angle and entry velocity.

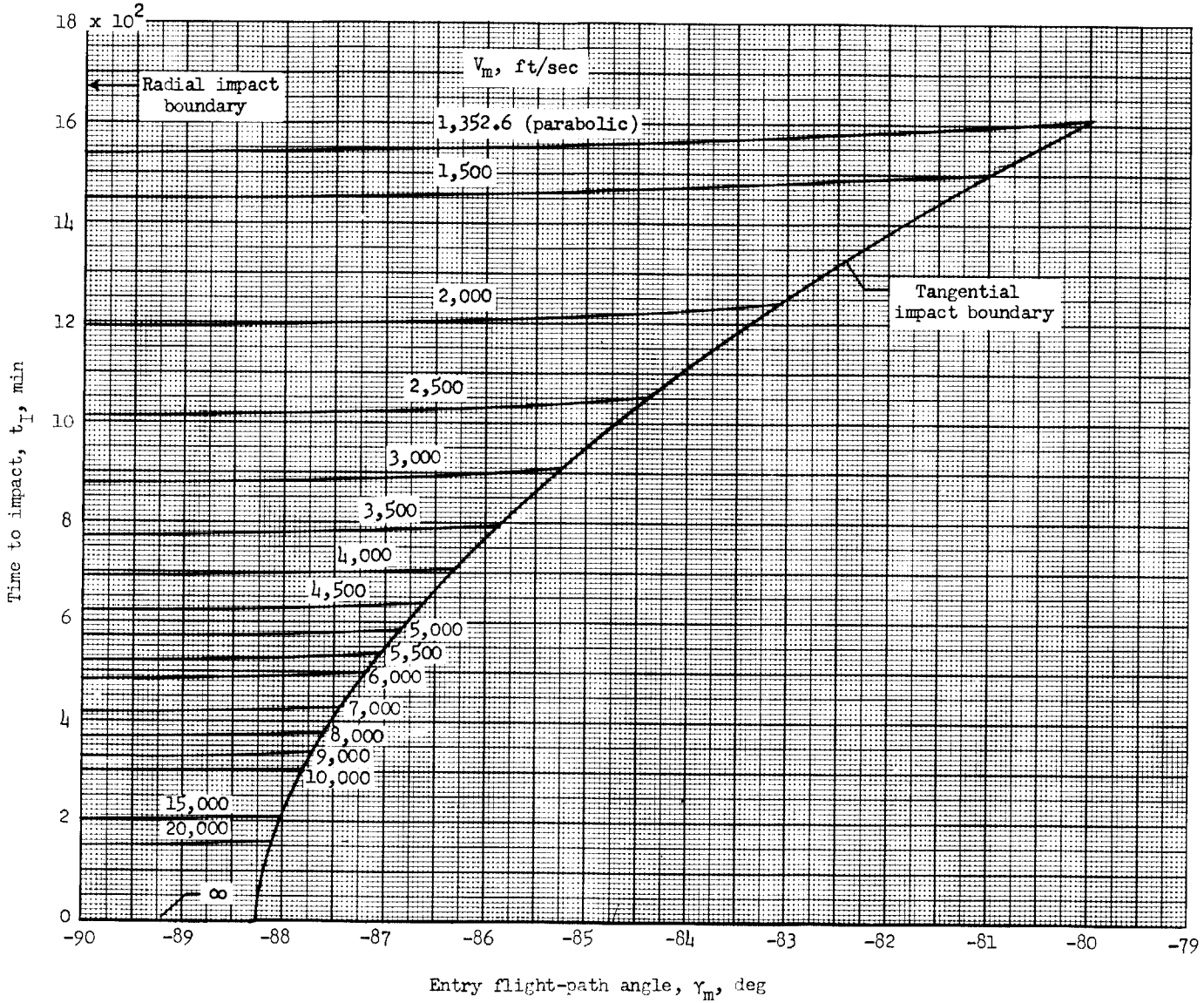

(a) Time to impact moon from altitude of sphere-of-influence surface.

Figure 15.- Variation of time to impact with entry flight-path angle and entry velocity.

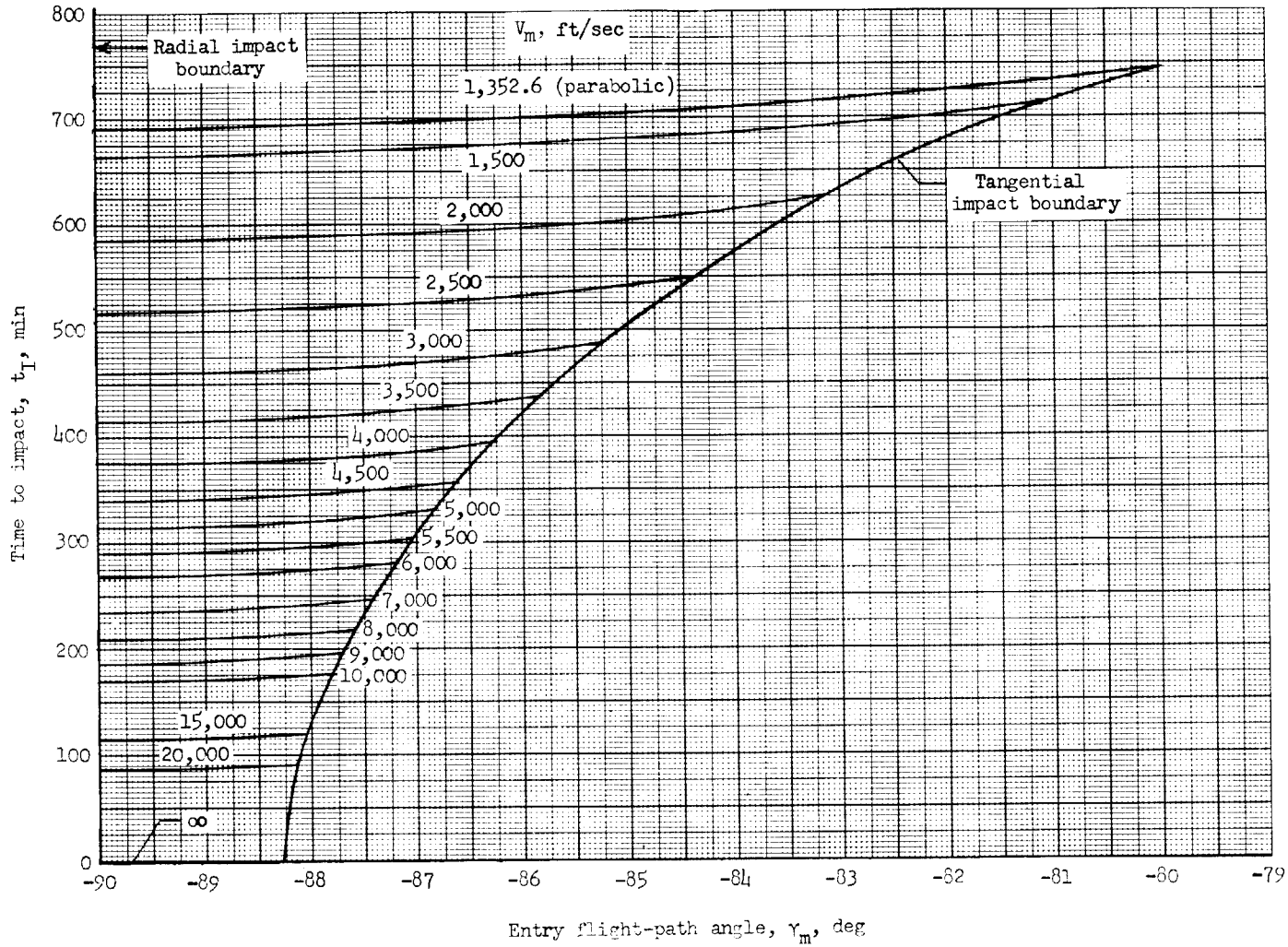

(b) Time to impact moon from altitude of 20,000 miles.

Figure 15.- Continued.

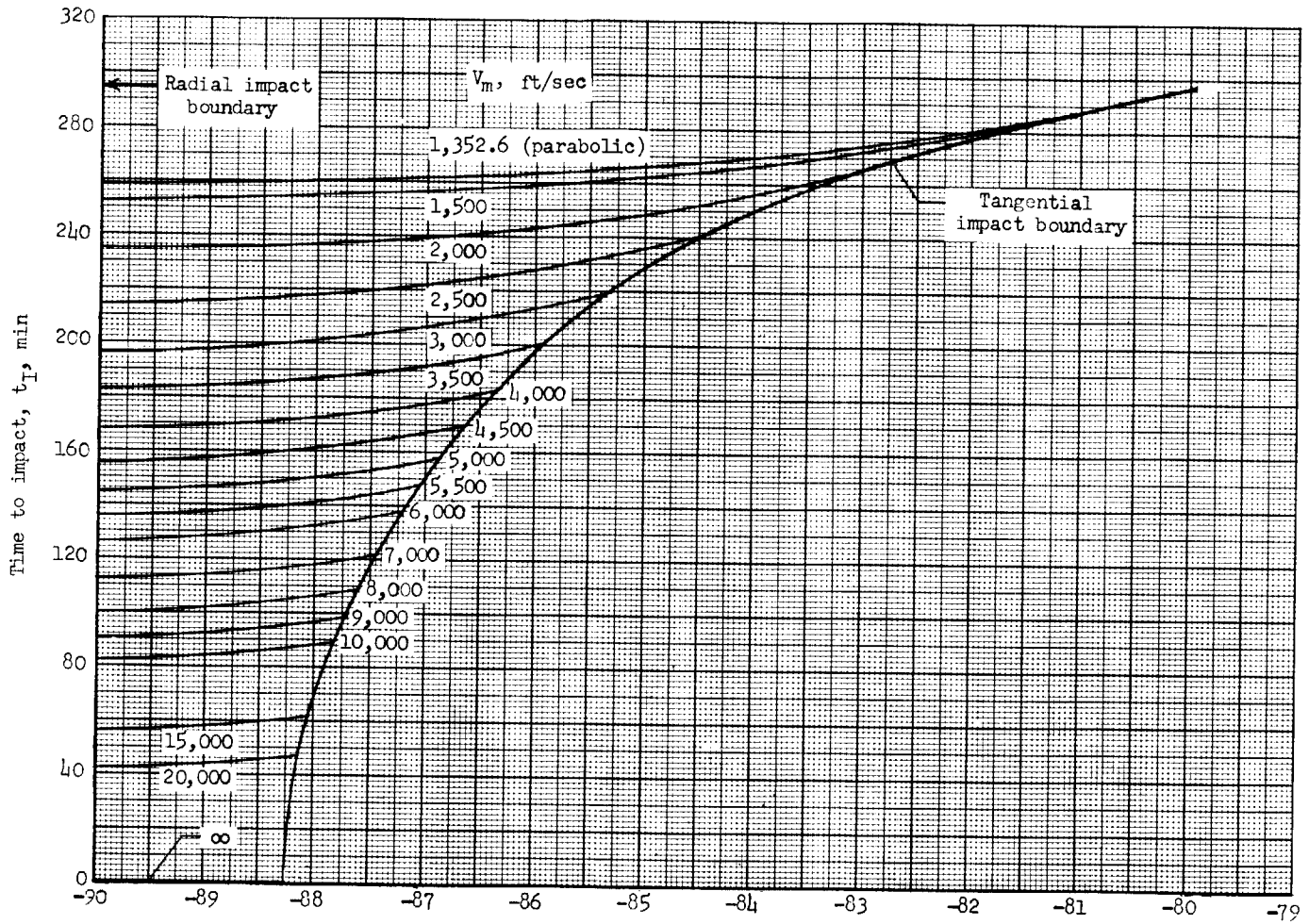

(c) Time to impact moon from altitude of 10,000 miles.

Figure 15.- Continued.

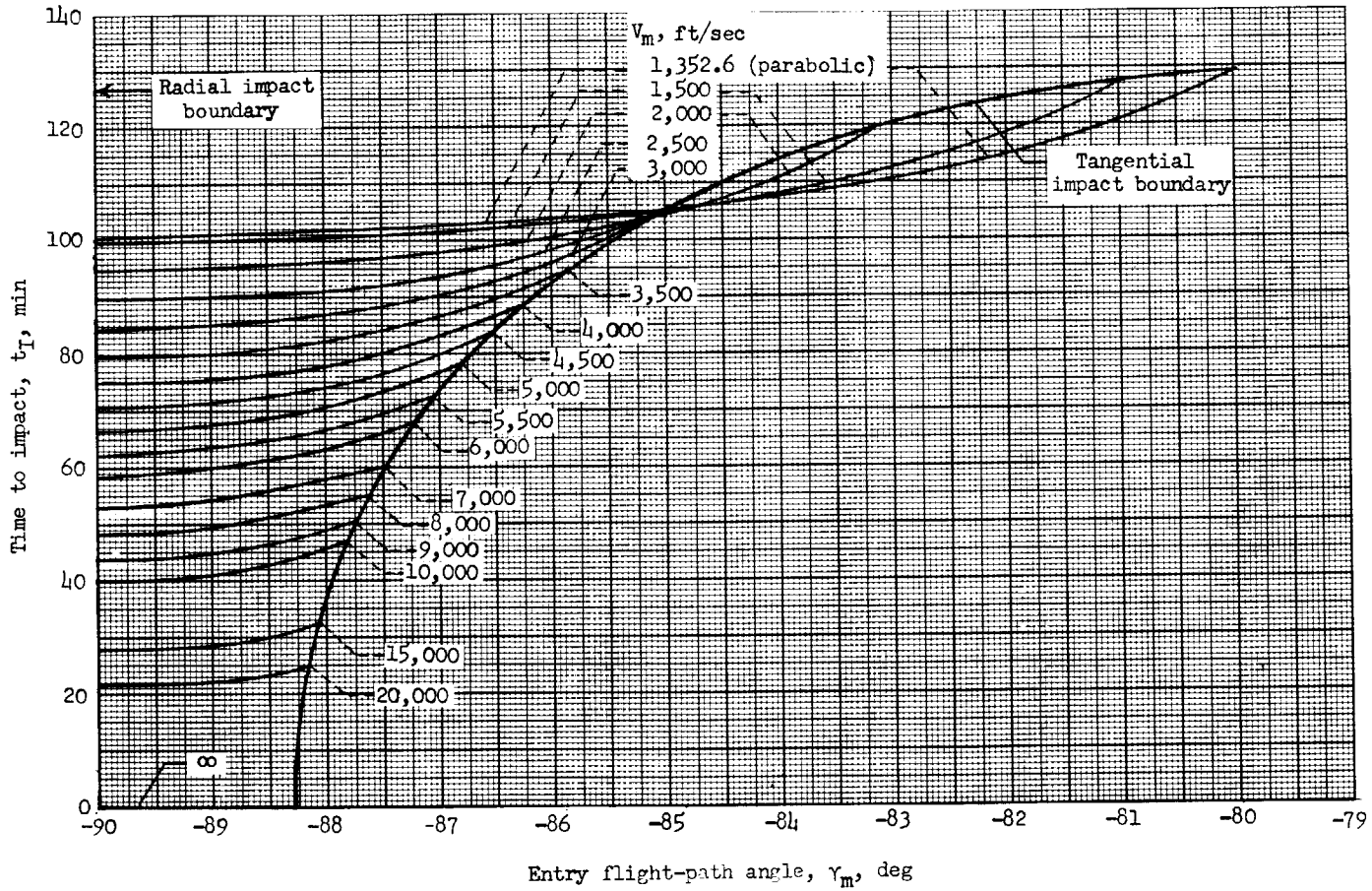

(d) Time to impact moon from altitude of 5,000 miles.

Figure 15.- Concluded.

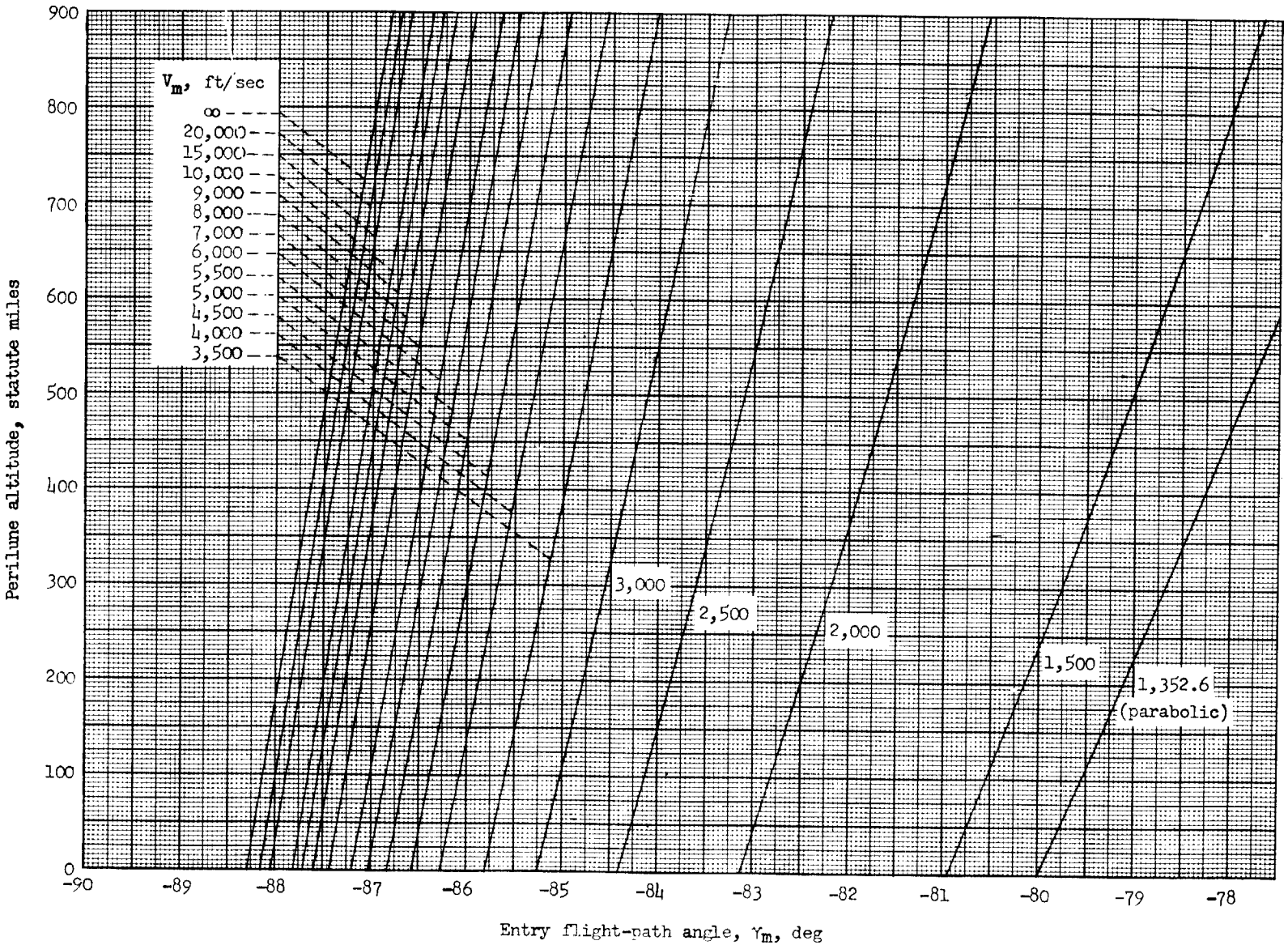

Figure 16.- Variation of perilune altitude (closest approach to lunar surface) with entry flight-path angle and entry velocity.

NASA-Langley, 1963